

C.P. No. 1329

C.P. No. 1329

LIBRARY
ROYAL AIR FORCE ESTABLISHMENT
BEDFORD.



PROCUREMENT EXECUTIVE, MINISTRY OF DEFENCE

AERONAUTICAL RESEARCH COUNCIL

CURRENT PAPERS

Urea Formaldehyde Foamed Plastic Emergency Arresters for Civil Aircraft

by

G. M. Gwynne

Engineering Physics Dept., R.A.E., Bedford

LONDON: HER MAJESTY'S STATIONERY OFFICE

1975

PRICE £2-20 NET

*CP No.1329
January, 1974

UREA FORMALDEHYDE FOAMED PLASTIC EMERGENCY ARRESTERS FOR CIVIL AIRCRAFT

by

G. M. Gwynne, B.Sc.

SUMMARY

This Report describes arresting trials with a Comet 3B aircraft at its maximum landing mass of 54400 kg at speeds up to 56 kn in test beds of urea formaldehyde foam of varying depth, length and density.

The main conclusions from the trials are that retardation of the aircraft in the arrester is independent of entry speed; significant drag is contributed by both the leading and trailing wheels of a bogie arrangement and this drag is predictable; the performance of the arrester is unaffected by the application of anti skid controlled wheel brakes; the foam causes no significant damage to turbine engines or aircraft structure; and the addition of a foam lead-in gradient to the full depth foam bed reduces the ratio of peak to mean retardation. A number of minor conclusions are also presented.

The Report includes design examples for foam arresters demonstrating that it should be possible to devise configurations, suitable for airfields where overrun hazards exist, for arresting aircraft safely without overstressing undercarriage units due to the foam drag loads.

CONTENTS

	<u>Page</u>
1 INTRODUCTION	3
2 THEORETICAL DESIGN CONSIDERATIONS	4
2.1 A wheel supported by the upper foam layer (Fig.1)	6
2.2 Wheel supported by both foam layers and protruding above the upper layer (Fig.2)	7
2.3 A wheel completely enveloped in the layers of foam (Fig.3)	8
2.4 Bogie wheels in foam (Fig.4)	8
2.5 Aircraft grouping	10
2.6 Undershooting aircraft	11
3 TRIALS WITH THE COMET 3B IN UF FOAM	11
3.1 Description of the foam beds	11
3.2 Instrumentation	13
4 RESULTS	13
5 DISCUSSION OF TRIALS AND RESULTS	14
5.1 Drag due to the application of wheel brakes	14
5.2 Vulnerability of the wheel brakes system	15
5.3 Ingestion of foam by the engines	15
5.4 Behaviour of bogie wheels in foam	16
5.5 Relationship between length of graded entry and drag	16
5.6 Off centre engagements	17
5.7 Movement of rescue vehicles on foam	17
5.8 Removal of the Comet from the foam arrester	18
5.9 Weatherproofing of foam arresters	18
5.10 Fire proof properties of foam	19
6 CONCLUSIONS	20
Appendix - Some examples of design investigation into the potential performance of foam arresters	23
Tables 1-6	30-41
References	42
Illustrations	Figures 1-27
Detachable abstract cards	-

1 INTRODUCTION

On average some 15 incidents of civil aircraft overrunning the ends of runways after an aborted take off or landing are reported to the International Civil Aviation Organisation each year. The incidents are reported from the major airports of the world, excluding those in the Iron Curtain countries, and in some cases have resulted in the death or serious injury of passengers and crew. Some airports have runways terminating relatively short distances from hazards such as busy roads, railway lines, embankments and abruptly falling ground. (Listed in the Appendix are the types of aircraft operating at such aerodromes, and Hong Kong, where the installation of soft ground arresters might be considered.)

With a soft ground arrester the braking force for stopping the aircraft is derived from the drag force exerted on the aircraft undercarriage as the wheels either displace, or shear and crush the soft ground material as they traverse through it. Gravel¹, aerated concrete, and sintered fuel ash pellets² are materials that have been considered for this purpose, but this Report deals only with Urea Formaldehyde (UF) foamed plastic manufactured by BIP Chemicals (Turner and Newall) Ltd, Oldbury, Worcester.

Previous reports on UF foamed plastic considered the feasibility of using this material³, and also the design of UF foamed plastic arresters for use by different groups of aircraft⁴. The only information available for formulating the latter report was based on results obtained from trials using a dummy Phantom aircraft. This aircraft of 17900kg mass was initially towed through blocks of foam to establish foam strength characteristics, and in later trials was catapulted into two 15.25m long by 3.05m wide pads of foam laid for engagement by the single wheels of the main undercarriage, in the speed range 60 to 100 kn.

The report however considered aircraft having undercarriages with single and multiple main wheels and maximum take off masses up to 322 000 kg. Typical dimensions for foamed plastic arresters for use at various airfields were suggested but, in arriving at the dimensions, many assumptions regarding the behaviour in general of bogie wheeled aircraft were made, the validity of which could only be verified or determined by trials. The present Report describes trials conducted to seek validation of these assumptions.

A time expired Comet 3B was made available for the trials and tests were carried out with this aircraft engaging test beds of foamed plastic of various lengths, depths, and density. The results obtained are reported.

Included in the Report (Appendix) are design examples of UF foamed plastic arresters based on the potential requirements for a number of United Kingdom airfields and Kai Tak airport at Hong Kong.

2 THEORETICAL DESIGN CONSIDERATIONS

Some of these aspects have been considered in an earlier report, but for the sake of clarity to the reader they are largely duplicated here, together with information made available as a result of the Comet trials.

The retarding force on an aircraft as its wheels traverse through foam is provided primarily by the crushing and shearing strength of the foam, which in turn varies according to its density. The strength of foam required for any particular aircraft can be assessed by considering the case where the arc of contact between the wheel and the foam is subjected to a uniform pressure acting radially. This pressure is unlikely to be a constant value over the entire arc of contact, but the value assumed is taken as representing the mean of the actual pressure distribution. From consideration of the vertical component of the aircraft's weight and the resulting foam pressure acting on the wheel, it will be seen that if the vertical component of weight exceeds the maximum upthrust pressure of the foam on the wheel, then the wheel will sink into the foam to a maximum depth, otherwise the wheel will seek an equilibrium position at a lesser depth. A consequence of this reduced penetration is a reduction in the drag force.

In order to obtain a worthwhile performance from the foamed plastic, the drag of the material must closely approach the design load strength of the aircraft's undercarriage.

To satisfy this requirement for both light and heavy-weight aircraft a two layer bed of foam is recommended, the upper layer being manufactured with a lower crushing strength foam. By adopting this method the depths of penetration of the wheels, drag and retardation become more proportional to aircraft weight and tyre size.

It is unlikely in a real arresting situation that a wheel will penetrate to its calculated depth and maintain this depth precisely throughout the arresting

run. This is due to minor inconsistencies in foam strength and variations in wheel loading arising from the aircraft motion. A variation in wheel depth will probably lead to a corresponding variation in the drag forces, and it is to be emphasized that it is the peak drag value which must be within the built in drag load strength of the undercarriage unit.

Lightweight aircraft which theoretically only partially penetrate the foam layers are more likely to experience drag changes due to wheel depth variations than heavier aircraft which produce full penetration of the foam bed.

From trials results the maximum crushable depth of the foam layers is 80% of the original depth, thereafter the foam becomes a consolidated layer under the wheel. Maximum values of retardation and drag occur when the aircraft enters the foam, and the drag value is largely dependent on the length of the foam lead-in gradient. Gradients of 1 in 12.5 produce a max/mean drag force ratio of between 1.3 and 1.4. Retardation values with foamed plastic are largely independent of aircraft engaging speed, and hence the undercarriage will be at risk if the undercarriage drag load strength is marginal, whether the entry speed is high or low.

The vertical components of aircraft weight on the nose and main undercarriage wheels are dependent upon the static loading of the aircraft, (i.e. its weight, and the fore and aft position of the CG) and also upon the weight transference from the main undercarriage to the nose undercarriage unit due to pitching caused by inertia forces generated as a consequence of the foam retarding forces on the main undercarriage. Detailed information on the geometry of some of the aircraft considered in the design examples was not readily available and for these it was assumed that the combined static and dynamic loads resulted in 15% of the aircraft's weight acting on the nose undercarriage and 85% on the main undercarriage. It was also assumed in all cases that the undercarriage load is shared equally between the wheels of each unit, and that the rolling radius of a tyre supported in foam is equal to its nominal undeflected radius.

The method outlined in this Report for determining depth of penetration by the wheels and undercarriage drag is essentially quasistatic. Initially the depth of penetration of the wheel is calculated by equating the vertical component of weight on the wheel to the vertical component of the tyre contact force, then with the wheel in this same position the horizontal component of the tyre contact force (the drag) is determined. Calculations of penetration depths

and drag require reference to Figs.1 to 4 which show four possible wheel conditions in foam that may be encountered. The first three cases refer to undercarriages with single or multiple wheels abreast and the fourth to bogie arrangements. When considering these cases the following notation will be used:-

W	=	vertical component of aircraft weight on a wheel
R	=	radius of a wheel
w	=	width of tyre
σ_1 and σ_2	=	mean effective crushing strengths of the upper and lower foam layers respectively
h_1 and h_2	=	depths penetrated by a leading wheel in the upper and lower foam layers respectively
h_3	=	additional depth penetrated by a rear bogie wheel
L_1 and L_2	=	depths of the upper and lower foam layers respectively
U	=	vertical component of foam upthrust pressure
D	=	foam drag
n	=	number of wheels crushing foam.

2.1 A wheel supported by the upper foam layer (Fig.1)

This case arises when the vertical component of aircraft weight on the wheel is insufficient to overcome the foam upthrust pressure of the layer, causing the wheel to seek an equilibrium position at a depth h_1 ($\leq R$) in the upper layer. The situation is akin to a wheel supported in a single layer of foam.

It is assumed that the foam exerts a uniform pressure over the arc of contact of the tyre with the uncrushed foam and that this pressure acts radially for each element of arc. The vertical component of this pressure termed the upthrust, is equal to the product of the tyre width, the mean crushing strength of the foam, and the horizontal projection of the arc AB of the tyre

$$U = w\sigma_1 BC$$

$$U = w\sigma_1 (2Rh_1 - h_1^2)^{\frac{1}{2}} \quad (1)$$

The foam drag on the tyre is the product of the tyre width, the mean crushing strength of the foam and the depth penetrated into the foam layer.

$$D = nw\sigma_1 h_1 \quad (2)$$

It can be seen from equation (1) that the maximum value of upthrust occurs when $h_1 = R$.

Then

$$U_{\max} = \sigma_1 w R \quad . \quad (3)$$

If the case of a wheel rolling in a single layer of foam is considered and the vertical component of aircraft weight W exceeds the maximum upthrust pressure value $\sigma_1 w R$, then the wheel will continue to sink into the foam until a consolidated layer of foam is formed under it. It is assumed that foam above axle height does not contribute to upthrust but the drag will increase from a value $\sigma_1 w h_1$ where $h_1 < R$ to a value $w \sigma_1 h_1$ where h_1 will equal the lesser of the two values $0.8L_1$ or $2R$.

Similarly in a double layer foam bed, when W exceeds $\sigma_1 w R$ the wheel will sink into the lower foam layer until either the upthrust from the combined layers equals the weight or a consolidated layer is formed under the wheel.

2.2 Wheel supported by both foam layers and protruding above the upper layer (Fig.2)

This case is a continuation of section 2.1 resulting from the vertical component of aircraft weight on the wheel (W) exceeding the upthrust pressure of the upper foam layer.

It is assumed as before that foam above wheel axle height does not contribute to upthrust, but does contribute to drag.

$$\text{Upthrust } U = \sigma_1 w C B - \sigma_1 w E D + \sigma_2 w E D$$

$$\begin{aligned} U &= \sigma_1 w \left[R^2 - (R - \overline{h_1 + h_2})^2 \right]^{\frac{1}{2}} - \sigma_1 w \left[R^2 - (R - h_2)^2 \right]^{\frac{1}{2}} \\ &\quad + \sigma_2 w \left[R^2 - (R - h_2)^2 \right]^{\frac{1}{2}} \\ U &= \sigma_1 w \left[R^2 - (R - \overline{h_1 + h_2})^2 \right]^{\frac{1}{2}} + w(\sigma_2 - \sigma_1)(2Rh_2 - h_2^2)^{\frac{1}{2}} \end{aligned} \quad (4)$$

or

$$U = w \left[\sigma_1 R + (\sigma_2 - \sigma_1)(2Rh_2 - h_2^2)^{\frac{1}{2}} \right] \quad \text{if } h_1 + h_2 \geq R \quad \text{or } h_2 \geq R. \quad (5)$$

Foam drag

$$D = nw(\sigma_2 h_2 + \sigma_1 h_1) \quad (6)$$

where

$$h_{2(\max)} = 0.8(L_1 + L_2) - L_1 \quad . \quad (7)$$

Substituting the wheel load value W for U in equations (4) or (5) when the mean crushing strengths of the foams are known determines the depths penetrated by the wheel; which substituted in equation (6) determines the drag. From equation (5) it will be seen that the maximum upthrust pressure of a double layer system occurs when $h_2 = R$ and has a value

$$U = \sigma_2 wR \quad . \quad (8)$$

2.3 A wheel completely enveloped in the layers of foam (Fig.3)

For this case the foam upthrust pressure equations are as shown in section 2.2, equation (5).

Foam drag

$$D = nw[\sigma_2 h_2 + \sigma_1 (2R - h_2)] \quad . \quad (9)$$

It will be observed that when a wheel is enveloped in foam that the foam above wheel height will contact the oleos and other undercarriage structures, producing in theory additional drag. It has been shown during trials with the Comet that this additional drag contribution due to interaction of foam with oleos, brake pipes and bogie structures can be neglected.

2.4 Bogie wheels in foam (Fig.4)

This case differs from the first three in that whilst four wheels exist on each main undercarriage unit to support and share the weight, the rear pair of bogie wheels by virtue of their position are constrained to roll in the furrows formed by the leading wheels. If the vertical component of weight on a leading wheel exceeds the maximum upthrust pressure of the foam bed (i.e. exceeds $\sigma_2 wR$), a consolidated foam layer is formed under it and further penetration and the production of drag by the rear wheel is prevented. Conversely if the weight on the leading wheels can be supported after partially crushing the foam layers, then the furrow so formed over the remaining uncrushed foam cannot support and prevent further penetration by the assumed equally loaded rear wheel. Additional drag is then produced.

If the latter case is now considered where drag forces are produced by both leading and rear bogie wheels then:-

Foam upthrust pressure U_1 on a leading wheel is given by

$$U_1 = \sigma_1 w \left[R^2 - (R - \overline{h_1 + h_2})^2 \right]^{\frac{1}{2}} + w(\sigma_2 - \sigma_1)(2Rh_2 - h_2^2)^{\frac{1}{2}} \quad (10)$$

or

$$U_1 = w \left[\sigma_1 R + (\sigma_2 - \sigma_1)(2Rh_2 - h_2^2)^{\frac{1}{2}} \right] \quad \text{if } h_1 + h_2 \geq R \quad (11)$$

Foam upthrust pressure U_2 on a rear bogie wheel is given by

$$U_2 = \sigma_2 w \left[2Rh_3 - h_3^2 \right]^{\frac{1}{2}} \quad \text{if } h_3 < R \quad (12)$$

or

$$U_2 = \sigma_2 w R \quad \text{if } h_3 \geq R \quad (13)$$

Foam drag D_1 on a leading wheel is given by

$$D_1 = nw(\sigma_2 h_2 + \sigma_1 h_1) \quad (14)$$

where $(h_1 + h_2)_{\max} = 2R$.

Foam drag D_2 on a rear wheel is given by

$$D_2 = n\sigma_2 w h_3 \quad (15)$$

Total drag on a bogie system is therefore

$$D = nw[\sigma_2(h_2 + h_3) + \sigma_1 h_1] \quad (16)$$

where

$$h_{3(\max)} = [0.8(L_1 + L_2) - (L_1 + h_2)] \quad (17)$$

To evaluate the depths h_1 , h_2 and h_3 the value of wheel load W is substituted for U_1 and U_2 in the appropriate equations.

Undercarriage wheel dimensions, loads, and configurations on any given group of aircraft are different, hence wheels penetrate the foam layers to differing depths. Calculation of wheel penetration depth and drag can therefore require the use of a combination of the equations (1) to (17).

2.5 Aircraft grouping

Derivation of the crushing strength required for a foam arrester requires consideration to be given to the aircraft types that are most likely to overrun the runway. Aircraft requiring say a 600m take off run compared with those requiring a 2000m take off run on the same runway are unlikely to overrun into the arrester after an emergency, due to the length of runway remaining in which to stop using wheel brakes alone. Attention can therefore be concentrated on the heavier and faster aircraft for determining the design strength requirements for the foam arrester. This policy tends to produce lower than optimum retardation values for the lighter and slower aircraft but in the event of complete brake failure, aerodynamic drag acting over the remaining runway length and foam drag should still be sufficient to stop them within the overrun area.

Attempts to establish the design criteria for foamed plastic arresters with the aircraft listed, whilst obtaining worthwhile values of retardation without overstressing the undercarriages, revealed that aircraft could be categorised into two groups, the grouping in both instances being dependent on the aircraft main undercarriage wheel unit configuration.

Group 1 - Aircraft with single or multiple main wheels abreast.

Group 2 - Aircraft with bogie undercarriages.

Group 1 aircraft generally require lower strength foam arresters than Group 2 which require additional strength and depth to ensure a drag contribution from the rear bogie wheels to produce adequate retardation.

Airports generally have both categories of aircraft using the same runways, and therefore all the operating aircraft cannot be arrested at an ideal value of retardation. The choice of arrester is likely to tend towards that which will give the greater protection, bearing in mind the frequency of operation of the major group; unless space exists in the overrun area for both types of arrester to be laid end to end.

2.6 Undershooting aircraft

Dynamic tests have not been carried out, but it is possible that an aircraft approaching the runway on a normal 3° glide path, still retaining lift on impact and thus reducing wheel loads, may impose no greater drag loads on the undercarriage than would occur in an undershoot on to a grassed area, or an overrun into a foam arrester with a 5° tapered entry. Drag loads arising from impact with soft ground or foam have received little attention, but work is being planned to investigate these to provide design data. Undershooting onto an arrester would however involve refoaming of the damaged sections.

3 TRIALS WITH THE COMET 3B IN UF FOAM

Seven engagements with the Comet, at its maximum landing mass of 54400 kg were carried out, in both simple and double layers of foam, at entry speeds in the range 36 kn to 56 kn. It was considered unnecessary to cover a wider range of engaging speeds, as trials with the dummy Phantom aircraft had shown that the retardation values in foam were largely unaffected by aircraft engaging speed. The objectives were to obtain further information on the following:-

- (i) Behaviour of bogie wheel arrangements in foam.
- (ii) Effect on arrester performance of applying wheel brakes controlled by an anti skid system.
- (iii) Maximum crushable depth of the foam layers.
- (iv) Drag attributable to the interaction of foam with oleos, brake pipes and bogie structures.
- (v) Vulnerability of the brake pipes situated between the wheels during arrests.
- (vi) Relationship between the length of the graded entry and the max/mean drag ratio.
- (vii) Methods of effectively sealing and weatherproofing the foam bed.

The test beds were situated on a runway to allow for a run-in and run-out distance of 425 m.

3.1 Description of the foam beds

Three pads of foam 30m long by 3.7m wide were laid for the first six runs, staggered so that nose and main unit wheels met foam resistance simultaneously Figs.5 and 6. In practice staggering of the arrester entry would not be feasible

as generally the wheel base dimensions of aircraft differ, neither can aircraft after emergencies be guaranteed to be on centre. During trials all engagements were on centre and staggering of the beds allowed the maximum amount of information to be derived from the full length of the test bed. Details of the foam test beds are in Table 1.

UF foam is manufactured on site, and pumped into position in liquid form where it rapidly hardens. Foam laying was carried out by representatives from BIP Chemicals Ltd, and with the equipment shown in Fig.7 a foam laying rate of approximately 0.5 cubic metre per minute was achieved.

Keying of the foam to the runway surface was accomplished by laying the foam on a matting of 50mm mesh steel wire 1.22m wide rawlbolted to the concrete, see Fig.8. An unmeshed section was left under the middle of each pad for easier removal of the powdery crushed foam after each aircraft engagement. Portable shuttering was used for controlling the width and height of the bed during foaming, allowing for approximately 8% and 3% shrinkage in depth and width respectively. The foam arrester was laid on firm level ground with adequate drainage. A direct relationship exists between the crushing strength of the foam and its density. During foam laying checks on the crushing strength of the foam were carried out at frequent intervals by means of simple density measurements. Containers of known mass and volume were filled with wet foam and weighed, from which the density was calculated and hence crushing strength determined. A further check on the strength was made when the foam had solidified using the device shown in Fig.9. This consisted of a rod of 25.4mm square section attached to the underside of a bathroom scale. Pressure applied on the surface of the scales to push in the rod to crush and shear the foam was directly displayed. Large variations in strength were observed for the foams laid for the first five engagements, necessitating removal and refoaming of the poorer sections. Tests conducted by the manufacturers indicated where deficiencies in control of the processes occurred and assurances were given that modifications would be incorporated when full scale foam making rigs were manufactured.

Requested mean crushing strength values of foam for use in trials in the upper and lower layers were 345 kPa and 585 kPa respectively. Measured strength values of the foams actually used are as shown in Table 2.

Repairs to the foam pads after each aircraft engagement involved the removal of the crushed foam (see Fig.10) and refilling the cleared ruts with new material.

Crushed foam was removed with shovels, the task being no more difficult than clearing crushed snow. New foam used for refilling does not form a bond with the existing foam, and to prevent it being dislodged by the aircraft wheels at the next engagement, the materials were keyed together by fluting the rut sides as shown in Fig.11.

3.2 Instrumentation

The parameters recorded during trials were aircraft speeds and retardations. Photographic recording of the engagements were made by means of cine cameras situated both on the aircraft and on the ground.

Aircraft speed was measured at entry into the foam bed using photoelectric devices situated on the runway connected to a microsecond timer, which displayed the time taken by the Comet to traverse the 1m separation between photocells. Comet speed on departure from the test bed was measured by a slit camera. This camera was run at constant speed and produced an image of the aircraft proportional in length to its speed. These entry and exit speeds provided a check on the average value of retardation during arrest.

Fitted axially on the floor of the aircraft passenger cabin above the CG position were three accelerometers, two $\pm 2g$ accelerometers manufactured by Shaevitz Ltd, and one $\pm 5g$ accelerometer of RAE design. The outputs of the former were recorded on an ultra violet light sensitive paper recorder using a 40Hz response galvanometer and of the latter on a photographic paper recorder with a 15Hz response galvanometer. The lower response galvanometer however was unable to record faithfully the transient retardation values in the early stages of the arrest.

Fitted under each wing and under the aircraft nose were 16mm cameras operating at 64 frames per second to record the behaviour of the wheels, but foam spray during the later runs tended to obliterate their field of view. Three ground based cameras were used to record the arrest, two 35mm high speed cameras situated 150m apart, one on each side of the foam bed and one 16mm camera situated 75 m in front of the bed on the edge of the runway.

4 RESULTS

Results obtained during the trials are presented in Table 1. Listed are:-

- (i) Values of aircraft speed measured on entry and departure from the test beds.

- (ii) Mean values of aircraft retardation throughout the arrest, calculated from the speeds and determined from the instrumentation records.
- (iii) Maximum values of retardation recorded.
- (iv) Mean retardation values recorded in the full depth foam bed and the values calculated from the performance equations. (Measured values were substituted for the mean crushing strength of the foam.)
- (v) Ratio of the recorded maximum to mean retardation values.

Theoretical and practical results are in good agreement, and show that the performance of a UF foam arrester is predictable.

5 DISCUSSION OF TRIALS AND RESULTS

It is to be noted that an optimised depth and strength of foam bed for use by the Comet was at no time intended. The depths and strengths of foam chosen were meant to simulate a range of conditions that could be encountered by aircraft in practice. The first three runs were carried out in a single layer of foam to seek confirmation of the predicted results set out in an earlier unpublished report. The test results largely confirmed the predictions. It was noticeable during these arrests that the nose wheels rode out of the arrester in the areas of detected high crushing strength foam. As in previous trials retardation values recorded were unaffected by variations in aircraft engaging speed, but were influenced by variations in the strengths of the foams laid. Maximum depths penetrated by the wheels before forming consolidated foam layers approximated to 80% of the original bed depth.

5.1 Drag due to the application of wheel brakes

An attempt to measure the additional drag produced by the application of wheel brakes during run No.3 was unsuccessful. A response time of 1.4 s was recorded from actuation of the foot brake to the achievement of full brake pressure. The aircraft in this time had travelled through the 30m long test bed. During the remaining runs wheel brakes controlled by a Maxaret Mk.2 anti skid system were applied 76 m from the test bed ensuring full brake pressure at entry. Retardation produced by wheel brakes alone was 0.28 g. Retardation traces recorded during an unbraked and a braked run are shown in Figs.12 and 13. It will be noticed that during the braked entry an initial 0.1s duration maximum value retardation pulse of 0.7 g was recorded, thereafter the retardation remained sensibly constant. The mean value over the constant portion was in

agreement with the value calculated for an equivalent unbraked run in a foam bed of the same strength. Wheel brakes therefore did not contribute additional drag during the foam arrest and from Fig.13 it can be seen that brake pressure released by the anti-skid system during the arrest was again not fully restored for a period of about 1.5 s after departure of the Comet from the test bed. It appears that on entering the foam bed, the friction between the tyre and the powdery crushed foam is so low that the wheel spins down under the action of the brake torque, causing the anti-skid system to release brake pressure. Full spin up has then not re-occurred until the tyre has contacted the high friction runway surface after departing from the test bed. This effect is advantageous to the foam arrester designer since the strength of the foam can be related to the safe working drag load strength of the undercarriage, as the only drag forces exerted are due to the foam, whether or not wheel brakes are applied. Although only one type of anti-skid system was used in tests there is no reason to assume that others would perform differently since all modern systems incorporate locked wheel protection. It is possible that in a long foam bed full wheel spin-up could occur causing re application of brake pressure, but, because of the low friction, very little brake torque would be developed before pressure would be released again.

5.2 Vulnerability of the wheel brakes system

The ability of the brake pipes situated between the bogie wheels and in front of the oleos to withstand a foam arrest without fracturing was in doubt. Steel plates were therefore manufactured and fitted between the wheels to protect the pipes. After run No.3 unpressurised brake pipes with standard connections were fitted on the front of the guards, thereby placing them in a more vulnerable position during arrests, Fig.14. No damage was seen or reported to either system during the remaining runs.

5.3 Ingestion of foam by the engines

To afford some protection to the engines, 50mm mesh steel wire guards were fitted over the four engine air intakes during trials to prevent ingestion of large foam fragments Fig.15. Observations made both during and after the runs revealed that a considerable quantity of foam had still been ingested by the engines without any apparent damage, Figs.16 and 17.

5.4 Behaviour of bogie wheels in foam

Retardation values recorded during the runs in the double layer foam were slightly greater than originally calculated, based on the assumption that the trailing wheels of the bogie would not contribute to drag⁴. Photographic evidence together with measurements of the depths of ruts formed by the main wheels revealed that the additional drag and retardation were produced by the rear bogie wheels, which had penetrated further than previously anticipated. The additional depth penetrated by these wheels was attributable to:-

- (a) The load on the leading wheels being insufficient to produce full penetration.
- (b) The base of the crushed foam rut formed by the passage of the leading wheels being incapable of supporting the assumed equally loaded rear wheels without undergoing further compression.

Recalculations made upon this basis for the mean retardation values were in good agreement with those recorded, which together with photographic views of the bogie attitude, lend credence to the bogie behaviour theory and performance equations in section 2.4. This agreement suggests that additional drag attributable to the interaction of foam with oleos, pairs of wheels on the same axle, brake pipes and bogie structures can be neglected. It is also considered that forces produced by the low mass fragmented foam impinging on these and other parts of the aircraft structure can be ignored.

5.5 Relationship between length of graded entry and drag

Maximum retardation values were recorded in the aircraft on entry into the full depth section of the foam bed. Foam lead in gradients of 1 in 10, 1 in 11, and 1 in 12.5 on the arrester prior to entry into the full depth section produced max/mean drag ratios of approximately 1.6, 1.5 and 1.35 respectively, therefore further decreases in the lead in gradient would appear beneficial. However, aircraft retardation whilst traversing the lead in gradient is small and whilst increasing the length of the graded entry reduces the max/mean drag ratio it also reduces the space available for laying the full depth section. When the distance available in the overrun area is limited a compromise choice has to be made. but it is recommended that at no time should a lead-in gradient steeper than 1 in 12.5 be laid. When constructing two layered foam beds, the lead in gradient should also be layered.

5.6 Off centre engagements

On completion of the first six runs, having established the behaviour of bogie wheel arrangements in foam and the effects of wheel brake application, the original programme was modified to include an investigation into:-

- (i) Aircraft behaviour throughout a full arrest.
- (ii) Subsequent removal of the Comet from the arrester.

A UF foam bed similar in strength to that used previously was laid, except that it was 90m long and foamed into one solid block to strengthen its structure. A mean retardation value of 0.54 g was calculated for the Comet from the measured crushing strength values of the foams laid.

During the seventh run, it was requested that the wheel brakes should be applied 76 m from the entry point, but due to a cross wind of 20 kn, gusting to 25 kn, differential wheel braking was required during the run into the arrester to retain directional control. The entry speed achieved was 47 kn, the aircraft stopping after traversing 55.5 m in the test bed with a recorded mean retardation of 0.47 g.

The aircraft entered the test bed 0.76m off centre to port at an angle of approximately 3° to the edge of the bed. The aircraft continued in this direction until the outer edge was reached, thereafter the wheels gradually returned into the main body of the arrester. The reduced value of retardation recorded is attributed to the lower than calculated value of drag on the port main undercarriage due to the shattering and weakening of the port edge of the bed by the wheels, as shown in Fig.18. The curved path followed by the wheels, Fig.19, also indicates that a greater value of drag was exerted on the starboard main wheels causing slight rotation of the aircraft to starboard. The pilot reported a smooth arrest. It may be concluded from the above that aircraft entering foam arresters at small angular offsets will be retained within the arrester but arrested at a somewhat lower value of retardation than calculated.

5.7 Movement of rescue vehicles on foam

Following the arrest of the Comet a fully laden Nubian Major fire fighting foam tender of 21300kg mass was driven up over the run out gradient on to the top of the foam bed, Fig.20. The front wheels rode over the surface of the foam without any appreciable penetration, whilst the rear wheels formed a rut approximately

0.075m deep. Foam arresters with upper layers having mean crushing strengths of 370 kPa and above will therefore not impede the movement of the heaviest of the present day rescue vehicles.

5.8 Removal of the Comet from the foam arrester

Prior to removal steel wire ropes of 690MN breaking load were lashed with nylon rope to the legs of each main undercarriage unit, Fig.21 and Fig.22 and to a steel wire purchase cable attached to a Scammel recovery vehicle. The aircraft was winched backwards through the uncleared crushed foam ruts, steering being controlled by a tractor sited on the foam bed and coupled to the nose wheel towing arm. The recovery operation took approximately 10 to 15 min after attachment of all ropes.

5.9 Weatherproofing of foam arresters

As mentioned previously UF foam is pumped into position and allowed to harden. Whilst possessing desirable compressive properties, it has weak tensile strength. During the curing period, due to different rates of cooling with shrinkage taking place, surface cracking of the foam bed occurs. Sealing and weatherproofing of the foam arrester is therefore essential to prevent damage by erosion.

The foam beds laid at Bedford were not in general weatherproofed or sealed, but in order that a weatherproofing method proposed by BIP Chemicals could be demonstrated, and its possible effect on the arresting performance ascertained a 12m length at the entry end of the 90m arrester was treated prior to run number seven.

A smooth foam surface was produced for sealing by the machine illustrated in Fig.23 which is basically an electrically powered transportable milling machine with traversing head. The foam surface was sealed by coating with a PVC emulsion paint over which was placed a layer of 0.33mm thick fibre glass cloth, which was also coated with two applications of the paint. Both PVC emulsion paint and fibre glass cloth were selected because they retain the fire proof properties of foam. The long term effectiveness of the materials used, and the method employed for weatherproofing cannot at this stage be guaranteed. Periodic inspection and maintenance on new installations would be most advisable. A fully weatherproofed foam pad is to be laid at Bedford and tests made to investigate the effects of jet engine blast.

5.10 Fire proof properties of foam

During an aircraft fire fighting exercise at Bedford the fire proof properties of UK foam were evaluated. Foam blocks were placed adjacent to the hulk of a Lightning aircraft, soaked with some 2000 litres of contaminated fuel oils and set alight. Tests made on the foam on completion of the fire fighting exercise revealed that surface charring of the foam only had taken place and that it was in no other way damaged.

Fire hazards exist whenever aircraft fuel tanks rupture. In the event of this occurring during a foam arrest, the spilt fuel will soak into the foam through the damaged weatherproofed skin. Whilst this will not prevent a fire starting it is conceivable that it will prevent a conflagration and the wide spread of flame.

5.11 Relative merits of various arresting systems

Comparisons between a foamed plastic arresting system and other prepared soft ground systems such as gravel, aerated concrete or sintered fuel ash pellets show that only in the former are performance characteristics predictable. During an aircraft engagement into a foamed plastic system there is no evidence that damage will be caused to vulnerable components such as brake pipes or turbine engines as a result of ingesting moderate quantities of the foam. Additionally, aircraft retardation values are independent of engaging speed and remain unaffected if wheel brakes controlled by an anti-wheel-locking device are applied.

Post installation work requirement for a foamed plastic system is minimal and comprises maintaining the weatherproofing skin in good order to prevent damage by erosion. Conversely gravel type systems require regular raking to prevent compaction. Repairs to an installation following an aircraft engagement may however be achieved more easily in the latter systems which merely require raking and levelling.

Hook cable arresting systems unlike the above cater for immediate resetting of the equipment and re-use of the runway; but suffer from the disadvantage of only being suitable for use by aircraft fitted with an arresting hook.

Arresting barrier systems may be engaged by both hooked and non-hooked aircraft but are incompatible with propeller driven types. Barrier nets have a 2 to 3 year life span when exposed to the elements and may only be used once without repair. A disadvantage of the system is that it is not under the direct control of the pilot, because it is brought to a state of readiness via the control tower.

6 CONCLUSIONS

As a result of the present series of trials with the Comet 3B aircraft the following conclusions may be drawn.

- (i) In agreement with earlier trials using the dummy Phantom aircraft, the retardation of the aircraft in the foam bed is independent of entry speed.
- (ii) With a bogie arrangement of undercarriage wheels significant drag is contributed by both the leading and trailing wheels.
- (iii) The drag on a bogie arrangement of wheels may be predicted with reasonable accuracy by the quasistatic method developed in this Report.
- (iv) In a representative arrester the maximum depth penetrated by the wheels before forming consolidated foam layers is approximately 80% of the original foam bed depth.
- (iv) The performance of the foam arrester is not affected by the application of wheel brakes controlled by an anti-skid system. The coefficient of friction between the tyres and the crushed powdery foam appears to be too low for significant brake torque to be developed. Consequently drag on the undercarriage units due to brake torque may be neglected.
- (iv) The drag due to interaction of the foam with the undercarriage oleos, brake pipes, bogie structures and to foam impingement on the aircraft structure may be ignored.
- (vii) There is no evidence of damage to vulnerable components such as brake pipes, or to the aircraft turbine engines resulting from the ingestion of moderate quantities of foam during an arrest.
- (viii) Peak drag force is developed in the foam on entry into the full depth section of the bed. The addition of an entry gradient reduces the ratio of the peak to mean retardation, this ratio decreasing with increasing length of the lead in. To maintain a ratio not exceeding approximately 1.3 the gradient should be less than 1 in 12.5.
- (ix) In cross winds of up to 25kn directional behaviour of the aircraft during an arrest presented no difficulties.
- (x) The removal of an arrested aircraft from a foam bed may be accomplished with conventional vehicles. Emergency service vehicles, including the largest fire tenders, can manoeuvre successfully on the foam bed.

- (xi) Aircraft entering foam beds at small angular off sets are unlikely to break out of the side of the arrester.
- (xii) The proposed method of sealing and weatherproofing the foam bed does not affect the performance of the arrester. The long term effectiveness of the materials used and the method of application has yet to be substantiated.
- (xiii) The presence of the foam does not add to the fire hazard existing during an emergency arrest, and may be beneficial in absorbing spilt fuel and inhibiting flame spread.
- (xiv) There may be a problem in the event of an aircraft undershooting the runway and landing on the foam arrester. Present evidence suggests that this should not increase the hazard above that already existing in an undershoot on to grass or soft ground. Work is being planned to investigate this aspect.
- (xv) The design examples included in the Report (Appendix) demonstrate that it should be possible to produce arrester configurations suitable for a number of airfields where such an installation might be considered. By appropriate design it is feasible to minimise the risk of undercarriage unit failure due to drag loads from the foam.

Appendix

SOME EXAMPLES OF DESIGN INVESTIGATION INTO THE POTENTIAL
PERFORMANCE OF FOAM ARRESTERS

The results of the trials reported here with the Comet and with the dummy Phantom, have served to establish the general performance and limitations of UF foam arresters, and to confirm the validity of the quasistatic theories used to determine the drag produced by single, multiple side-by-side, and bogie undercarriage arrangements.

It is not the function of the RAE to act as Design Authority for foam arrester systems and it is anticipated that the detail design of arresters will be conducted by contractors in consultations with the Airport Authorities involved. However, to assist potential designers, it has been thought useful to incorporate in this Report some examples which may clarify the process. Although the design examples relate to actual airfields and the types of aircraft operated from them, it must be emphasised that the resulting configurations of arresters do not constitute recommendations. In particular the information on aircraft performance and undercarriage design ultimate load strengths quoted in this Appendix, should not be used without confirmation from the aircraft constructors, since these figures are likely to change with development of the aircraft.

Foamed plastic arresters should ideally be designed to cater for the needs of each individual airport. For each airport the designer should examine the range of aircraft operated and from the aircraft constructors data obtain the following information:-

- (i) The ultimate drag force that can be applied to the undercarriage units of each aircraft.
- (ii) Tyre sizes and wheel unit configurations.
- (iii) Aircraft mass; and details of their geometry for the evaluation of wheel loads.

As stated previously the depths of penetration of aircraft wheels into foam are dependent on the loads on the undercarriage which in turn vary according to the overall weight of the aircraft. When assessing the performance of a foam bed for a particular aircraft, three weight states should be considered namely

(i) maximum take off (ii) maximum landing and (iii) a typical minimum operating weight. The two former values are readily obtainable whilst the latter can only be estimated; a typical value being obtained based on the sum of the following:-

- (a) Aircraft operational weight empty.
- (b) 25% of payload.
- (c) An amount of fuel for a 45 minute diversion on arrival at an airport.

Values for the crushing strengths and depths of the foam layers are obtained by a method of successive approximation, and for this, reference is made to equation (3) of section 2.1, which states

$$U_{\max} = \sigma_1 wR \quad . \quad (3)$$

If the values of wheel loads calculated at the estimated minimum weight of the aircraft operating at an airport are substituted for U_{\max} in equation (3) a series of values for σ_1 will be obtained, from which the first approximated mean value for σ_1 the crushing strength of the upper foam layer can be obtained. Similarly by substituting the wheel load values calculated at the aircraft's maximum take off weight for U_{\max} in equation (8) an approximated mean value for σ_2 , the crushing strength of the lower layer may be obtained.

Adopting the procedures outlined in section 2.1 to 2.4 in calculating undercarriage drag values for successive selections of foam depths and strengths ensuring that undercarriage drag loads are not exceeded for the selected aircraft, produces the final choice.

A.1 United Kingdom airfields

The range of aircraft operated from the UK airfields is shown in Table A2, although each airfield only serves certain aircraft in the range. Observation of aircraft movements at a number of UK airfields where such an installation might be considered indicated that the BAC 1-11 and Viscount 700 are the two major users. Accordingly, as an example, the design strength of an arrester potentially suitable for such airfields has been chosen so as not to over stress these undercarriages. For such designs an upper foam layer 0.30m deep with a mean crushing strength of 210 kPa laid over a 0.38m deep foam layer with a mean crushing strength of 415 kPa is considered. Overall lengths of the arrester have not been stated, as these values are dependent on the actual length available in the overrun area, and on whether some of the existing runway surface can be covered with foam for increasing overall arrester lengths and

hence their effectiveness. However the configuration shown in Fig.24 can be regarded as an example of a possibly suitable representative arrester.

Calculated values of combined static and dynamic wheel loads, undercarriage drag forces and retardations based on the UF arrester dimensions are listed in Table 3. The drag forces and retardation values quoted are mean values. Trials have shown that a max/mean drag force ratio of 1.3 is probable. If a soft ground type of arrester were intended for routine use, say on each landing, the ratio of undercarriage design ultimate drag load strength to mean drag imposed would normally have a minimum value of 3.0. However, the foam arrester is solely intended for emergency use and a value of 2.0 for this ratio is considered reasonable.

Table 4 lists the undercarriage design ultimate drag load values, calculated mean drag load values, and their ratios for a selection of British aircraft. The ultimate drag load values quoted are manufacturer's values for high drag landing cases, where undercarriage oleos are fully extended and the bending moments are at a maximum. With the undercarriage units at near static closure as would probably occur in most overrun cases, greater drag loads can be sustained. For example the high drag landing design ultimate drag load value for the Trident 2E nose wheel is 112 kN whilst for the dynamic braking case the value is 156 kN.

Ratios of design ultimate drag to calculated mean drag load values of less than 2.0 indicate a possibility, but not a certainty, of undercarriage failure. It should be noted that the risk is independent of the engaging speed. Nose pitching and slewing of tail wheeled aircraft such as the Bristol 170 and the DC3 is another possibility during arrests.

After examination of the dimensions selected for the UK foam arrester it can be seen that increases made to the foam depth and strength would be advantageous for increasing the retardation values for some of the heavier and faster aircraft, especially aircraft of the Group 2 category. The frequency of operation of these aircraft, coupled with the maximum drag load value that can be applied to the BAC 1-11 nose undercarriage limited the choice of dimensions to those stated. Lighter aircraft, for example the Britten Norman Islander, would benefit by a reduction in the foam crushing strength, permitting deeper penetration by the wheels and increases in drag loads. These aircraft however require much shorter take off runs than say the BAC 1-11, and their probability of overrunning at high speeds seems slight, therefore again not

warranting alteration of the foam arrester dimensions. When determining and estimating the performance for a selected length of this particular arrester reference should be made to Fig.27 and the table showing the retardations calculated for aircraft operating at the airport. For example consider an airport where BAC 1-11 Series 200 and Comet 4 aircraft are operated, and suppose the performance of a full depth foam bed of 75m length has to be investigated. From Table 3 it is seen that a BAC 1-11 Series 200 at maximum landing weight has a mean retardation of 0.85 g and from Fig.27 that an aircraft with this retardation can be brought to rest from speeds of up to 69 kn. Similarly the Comet 4 at maximum landing weight with a mean retardation of 0.45 g will be brought to rest from speeds of up to 50 kn. Increasing the foam arrester length by 30m to 105m total, would then cater for the same two aircraft at entry speeds up to 81.5 kn and 59.5 kn respectively.

Full retardation is not achieved until all wheels are in the foam bed. Therefore in calculating the overall length of a foam arrester, the wheel base length and the foam graded entry length must be added to the stopping distance.

A.2 Hong Kong airport (Table A1)

At this airport an overrun length of approximately 250 m is potentially available and the operating aircraft listed in Table A3 have all up masses in the range 10900 kg to 322 000 kg. No single uniform foam arrester capable of arresting all the aircraft at a worthwhile value of retardation seems possible. Both categories of aircraft operate at the airport, but greater concern has been expressed by the authorities over the stopping of overrunning Group 2 aircraft and the Boeing 747 in particular. Designing an arrester solely for these aircraft would in all probability result in an arrester capable of overstressing the undercarriages of Tridents and other aircraft of the Group 1 category at any entry speed. An attempt at a compromise suggested the installation of two arresters laid end to end, the first arrester ensuring the safe arrest of Group 1 aircraft, their maximum safe overrun entry speed being then solely dependent upon the length of the bed and the retardation generated.

A typical example illustrated in Fig.25 considers an initial single layer bed of foam 61m long, 0.685m deep with a mean crushing strength of 345 kPa, laid in front of a double layered foam arrester with an upper layer 0.51m deep of 380kPa mean crushing strength, over a layer 0.635m deep of 760kPa mean crushing strength foam. Calculated values of drag and retardation for a selection of

the operating aircraft in the single and double layered foam arresters are listed in Tables 5 and 6 respectively.

It will be seen from Fig.27 that with the retardation calculated and the length selected for the first arrester, that the maximum safe overrun entry speed for the Trident at its maximum landing weight is 57 kn. Higher entry speeds would result in the aircraft entering the second harder arrester with the likelihood of undercarriage failure. Loss of the nose undercarriage only may not be hazardous for the nose would probably slide on the foam and the aircraft maintain its directional stability. The first foam arrester consisting of a single layer is chosen in preference to the UK double layered foam arrester as comparisons made of the retardation values calculated for the aircraft in the upper weight range of Group 1 operating at the airport differed only slightly, whilst the work load in laying a single layer will be greatly reduced.

Details of the overall foam arrester layout and the overrun area available are shown in Figs.25 and 26. It will be noticed that lead-in gradients between arresters have been retained and that the maximum length available has been used. Approach lights and localizer aeriels would require modification, possibly being installed on frangible pillars to reduce aircraft damage in the worst overrun cases.

In order to provide easier access for emergency services to an arrested aircraft from any point alongside the foam beds, ramping of the arrester sides with foam or soil with a turfed surface could be employed. The choice of the latter would be advantageous in preventing lifting of the weatherproofed beds by typhoons, but could be more hazardous than the former to aircraft attempting to break out of the side of the arrester.

The ground below the arrester should be firm and level, existing turf should be removed and hardcore rolled in. Due to the proposed size of the arrester and ramping of the sides, keying of the foam to the overrun surface would only be required at the graded entry end.

Table A1

Details of Hong Kong airport

Hong Kong R/W 13/31 length 2545 m

- (a) Depth of water table Runway level + 5.7m above PD (Port Datum) tidal range 0.00 PD to + 4m PD. Therefore water table could be exceptionally up to 1.5m below ground level. Normal is approximately 3.0m below ground level.
- (b) Type of soil This varies across the site from solid rock, approximately 1.5m to 3m below ground level, to granular fill (i.e. decomposed granite) with rockplums (varying sizes). There is also an old watercourse which may have variable fill, detritus etc.
- (c) Services etc. in site area All services skirt the area which may be used for the arrester device site.

The space available for an arrester bed is 183 m × 90 m if set up behind the ILS or 250 m × 90 m if the localiser could be set on top of the bed.

Critical aircraft - B747, entry speed $V_1 = 158$ kn at mass 322 000 kg.

- (d) One end of the runway terminates in the sea, the other terminated 300 m from a densely populated tenement area.

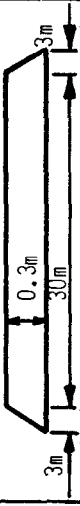
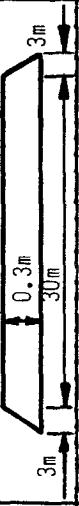
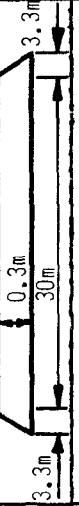


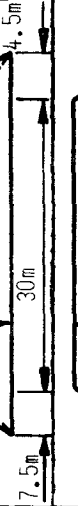
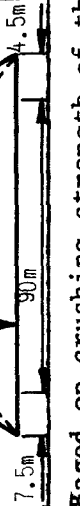
Table A 2Details and category of aircraft operating at applicable UK airports

Group 1	Group 2
Dove	Comet 4
Heron	Douglas DC 8 SRS 10
Apache/Aztec	Douglas DC 8 Super 63
Beagle 206 SRS 1 and 2	Brittania 300
Britten Norman Islander	Boeing 707/320B
Britten Norman Trilander	Boeing 720
Douglas DC 4	Boeing 720B
Douglas DC 3	
Bristol 170	
Viscount 700	
Viscount 700D/800	
BAC 1-11 SRS 200	
BAC 1-11 SRS 300/400	
BAC 1-11 SRS 500	
Boeing 737 SRS 200	
Nord 262	
Carvair	
Herald 700	
Vanguard 953	
Vanguard 951	
Argosy	
Hawker Siddeley 125	
Hawker Siddeley 748	

Table A3Details and category of aircraft operating at Kai Tak airport Hong Kong

Group 1	Group 2
Douglas DC 4	Super VC 10
Douglas DC 9 SRS 10	Boeing 707 SRS 120B
Douglas DC 9 SRS 40	Boeing 707 SRS 320C
DHC 4A	Boeing 720 SRS 720
Jetstream	Boeing 720 SRS 720B
Viscount 700	Brittania
Boeing 727 SRS 100A	Convair 880 SRS 22
Boeing 727 SRS 200	Convair 880 SRS 22M
Boeing 737 SRS 100	Convair 990A
Boeing 737 SRS 200	Douglas DC 8 SRS 10
Douglas DC 3	Douglas DC 8 Super 63
Trident 2E	Boeing 747

Table 1
RESULTS FROM TRIALS WITH COMET 3B IN FOAMED PLASTIC

Run No.	Foamed plastic test bed size	Aircraft speeds		Calculated mean retardations from speeds g	Recorded values of retardation g			* Calculated mean retardation in the full depth section g	Max Mean Col.7 Col.8
		Entry into test bed kn	Departure from test bed kn		Overall mean	Maximum	Mean in the full depth section		
1		36.75	27.5	0.22	0.22	0.3	0.22	1.36	
2		49.5	41.7	0.26	0.26	0.44	0.27	1.63	
3		53.5	46.0	0.26	0.26	0.43	0.28	1.48	
4		43.6	26.9	0.37	0.37	0.53	0.44	1.18	
5		55.4	38.1	0.51	0.50	0.70	0.49	1.37	
6		49.0	26.2	0.54	0.53	0.71	0.51	1.34	
7		47.0		0.47	0.47	0.63	0.54	1.36	

* Based on crushing strength of the foamed plastic laid.

Table 2

MEASURED MEAN CRUSHING STRENGTH VALUES OF
UREA FORMALDEHYDE FOAM USED FOR TRIALS

Run No.	Nose bed		Port main wheel bed		Starboard main wheel bed	
	Upper layer kPa	Lower layer kPa	Upper layer kPa	Lower layer kPa	Upper layer kPa	Lower layer kPa
1	-	large scatter	-	large scatter	-	large scatter
2	-	648	-	496	-	524
3	-	648	-	552	-	510
4	331	641	290	524	262	579
5	248	593	296	648	283	607
6	310	627	317	600	338	614
7	386	586	372	641	386	614

N.B. The nominally specified values for the upper and lower layers were 345 kPa and 585 kPa respectively.

Table 3

DETAILS OF AIRCRAFT OPERATING AT UK AIRFIELDS AND THEIR CALCULATED DRAG AND MEAN
RETARDATIONS IN A PLASTIC FOAM ARRESTER 0.30m DEEP x 210kPa FOAM OVER
0.38m DEEP x 415kPa MEAN CRUSHING STRESS FOAM

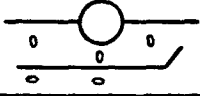
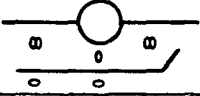
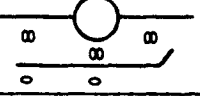
Aircraft	Maximum aircraft mass		Undercarriage type	Tyre sizes		Dynamic wheel loads		Calculated drag		Total drag kN	Retardation G	
	Take-off kg	Landing kg		Nose wheel	Main wheel	Nose kg	Main kg	Nose unit kN	Main unit kN		Take-off mass	Landing mass
Dove	4100	3900		18.5 x 7	27 x 8.75	580	1640	2.1	28.0	30.1	0.77	0.80
						610	1730	2.4	28.2	30.6		
Heron	6100	5900	As above	20 x 8	29 x 9.25	890	2540	4.6	35.2	39.9	0.69	0.68
						920	2600	4.9	36.4	41.3		
Apache	2200	2200	As above	17.25 x 6	18.25 x 7	330	930	0.8	22.5	23.3	1.03	1.09
Aztec	2350	2350				350	1000	0.9	22.8	23.7		
SRS 1	3400	3250	As above	17.25 x 6	24 x 7.5	480	1370	1.9	24.4	26.3	0.81	0.83
Beagle 206 SRS 2	3400	3250				510	1450	2.1	24.8	26.9		
BN Islander	2700	2700		17.25 x 6	17.25 x 6	400	580	1.3	11.9	13.2	0.49	0.49
						400	580	1.3	11.9	13.2		
BN Trilander	4200	4200	As above	18.5 x 6.75	18.5 x 6.75	640	900	2.8	43.4	46.2	1.11	1.11
						640	900	2.8	43.4	46.2		
DC 4	33100	28800	As above	45 x 16.25	45 x 15.5	4320	6120	24.6	115.2	139.8	0.53	0.50
						4320	7040	26.0	145.5	171.5		
HS 748	20200	18800		25.65 x 8.5	32 x 10.75	1410	4000	20.2	123.0	143.2	0.90	0.78
						1510	4290	27.2	151.0	178.2		
Viscount 700D/800	29300	26500	As above	24 x 7.25	36 x 10.75	1990	5640	35.7	179.0	214.7	0.78	0.83
						2190	6220	45.4	179.0	224.4		

Table 3 (continued)

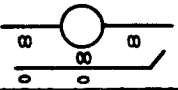
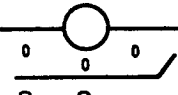
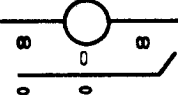
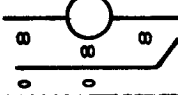
Aircraft	Maximum aircraft mass		Undercarriage type	Tyre sizes		Dynamic wheel loads		Calculated drag		Total drag kN	Retardation G	
	Take-off kg	Landing kg		Nose wheel	Main wheel	Nose kg	Main kg	Nose unit kN	Main unit kN		Take off mass	Landing mass
Viscount 700	29300	24500		24 × 7.25	36 × 10.75	1840	5210	30.9	179.0	209.9	0.78	0.87
						2190	6220	45.4	179.0	224.4		
BAC 1-11 200	35600	31300	As above	24 × 7.25	40 × 12	2350	6650	60.4	199.9	260.3	0.75	0.85
BAC 1-11 300/400	39500	35400	As above	24 × 7.25	40 × 12	2650	7520	60.4	199.9	260.3	0.67	0.75
BAC 1-11 500	41300	38100	As above	24 × 7.25	40 × 12	2860	8100	60.4	199.9	260.3	0.64	0.70
Boeing 737/200	48500	44000	As above	24 × 7.7	40 × 14	3300	9350	64.1	233.1	297.2	0.62	0.69
						3640	10300	64.1	233.1	297.2		
Nord 262	10600	10300		22 × 9	38 × 12.5	1550	4380	14.7	48.3	63.0	0.63	0.62
						1590	4510	14.8	50.3	65.1		
Carvair	33500	29100		44 × 16	45 × 15.5	4370	6190	25.6	116.8	142.4	0.53	0.50
						5020	7110	25.7	148.9	174.6		
Herald 700	19500	17900		23 × 7.25	34 × 11.75	1340	3810	24.0	93.1	117.1	0.69	0.67
						1460	4150	25.1	107.0	132.1		
Vanguard 953	64400	59200	As above	35 × 9.75	49 × 17	4440	12580	81.2	283.1	364.3	0.58	0.63
						4830	13690	81.2	283.1	364.3		
Vanguard 951	61200	52800	As above	35 × 9.75	49 × 17	3960	11200	57.9	283.1	341.0	0.61	0.66

Table 3 (concluded)

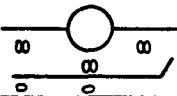
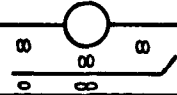
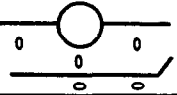
Aircraft	Maximum aircraft mass		Undercarriage type	Tyre sizes		Dynamic wheel loads		Calculated drag		Total drag kN	Retardation G	
	Take-off kg	Landing kg		Nose wheel	Main wheel	Nose kg	Main kg	Nose unit kN	Main unit kN		Take off mass	Landing mass
HS 125	10500	9050		18 x 4.25	23 x 7	680 790	1920 2250	14.6 16.6	74.9 116.6	89.5 133.2	1.29	1.01
Argosy	42200	40100	As above	32 x 10.75	45 x 15.5	3010 3160	8530 8960	38.3 40.3	247.0 258.1	285.3 298.4	0.72	0.72
Comet 4	73500	54400		30 x 9	36 x 10	4080 5510	5780 7810	74.9 74.9	166.5 166.5	241.4 241.4	0.34	0.45
DC 8 SRS 10	124000	87500	As above	34 x 11	44 x 16	6570 9290	9300 13160	91.6 91.6	266.6 266.6	358.2 358.2	0.29	0.42
DC 8 Super 63	158800	111100	As above	34 x 11	44 x 16	8340 11910	11810 16870	91.6 91.6	266.6 266.6	358.2 358.2	0.23	0.33
Brittania 300	83900	63500	As above	32 x 8.8	40 x 12	4760 8390	6750 8920	73.3 73.3	199.8 199.8	273.1 273.1	0.33	0.44
Boeing 707/320B	148300	93900	As above	39 x 13	46 x 16	7040 11130	9980 15760	108.2 108.2	266.5 266.5	374.7 374.7	0.26	0.41
720 Boeing 720B	103900 103900	79400 79400	As above	34 x 9.9	40 x 14	7770 5950 7960	11030 8430 11280	82.4 82.4	233.1 233.1	315.5 315.5	0.31	0.41
Bristol 170	19900	19900		-	45 x 15.5	-	9980 9980	-	129.1 129.1	129.1 129.1	0.66	0.66
DC 3	11400	10900	As above	-	45 x 17	-	5440 5700	-	54.7 55.4	54.7 55.4	0.49	0.51

Table 4

AIRCRAFT UNDERCARRIAGE DESIGN ULTIMATE LOAD STRENGTHS AND CALCULATED DRAG LOADS

(from Table 3)

Aircraft	Nose wheel unit			Main wheel unit		
	Design ultimate drag (high drag landing)	Drag in UK example foam bed	<u>Ult. drag</u> foam drag	Design ultimate drag (high drag landing)	Drag in UK example foam bed	<u>Ult. drag</u> foam drag
	kN	kN	-	kN	kN	-
BAC 1-11 series 500	117.9	60.4	1.95	279	99.9	2.8
Comet 4	118.1	74.9	1.6	573.8	83.3	6.9
Britten-Norman Islander	12.8	1.3	9.8	24.5	5.9	4.2
Heron	18.1	4.9	3.7	58.7	18.2	3.3
Dove	18.7	2.4	7.8	39.8	14.1	2.8
Viscount 700	105.6	45.4	2.3	200.1	89.5	2.2
Viscount 700D/800	119.7	45.4	2.6	229.1	89.5	2.6
Vanguard 953	179.0	81.2	2.2	412.6	141.6	2.9
Bristol 170	-	-	-	141.3	64.5	2.2
Brittania 300	167.1	73.3	2.3	477.3	99.9	4.8
Carvair	54.7	25.7	2.1	213.1	74.5	2.9
Herald 700	65.8	25.1	2.6	122.8	53.5	2.3
HS 125	36.3	16.6	2.2	91.8	58.3	1.6
Argosy	197.0	40.3	4.9	292.2	129.0	2.3
HS 748	77.4	27.2	2.8	143.2	75.4	1.9
Trident 2E	112.0	-	-	415.0	-	-

Table 5

DETAILS OF AIRCRAFT OPERATING AT 'HONG KONG' AND THEIR CALCULATED DRAG AND MEAN RETARDATION
IN A PLASTIC FOAM ARRESTER BED 0.68m DEEP × 345kPa MEAN CRUSHING STRESS FOAM

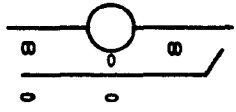
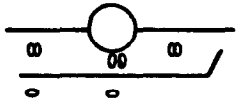
Aircraft	Maximum aircraft mass		Undercarriage type	Tyre sizes		Dynamic wheel loads		Calculated drag		Total drag kN	Retardation G	
	Take-off kg	Landing kg		Nose wheel	Main wheel	Nose kg	Main kg	Nose unit kN	Main unit kN		Take-off mass	Landing mass
DC 4	33100	28800		45 × 16.25	45 × 15.5	4320 4970	6120 7040	11.9 16.2	113.7 168.5	125.6 184.7	0.57	0.44
DC 9 SRS 10	35200	33600		26 × 6.6	40 × 14	2520 2640	7130 7490	63.4 63.4	269.0 269.0	332.4 332.4	0.96	1.01
DC 9 SRS 40	51700	46300	As above	26 × 6.6	40 × 14	3470 3880	9830 10990	63.4 63.4	269.0 269.0	332.4 332.4	0.66	0.73
DHC-4A	12900	12900	As above	24 × 7.5	32 × 11	969 969	2750 2750	4.8 4.8	43.0 43.0	47.8 47.8	0.38	0.38
Jetstream	19100	15800	As above	18 × 4.4	26 × 6.6	1190 1430	3370 4050	35.2 35.2	126.8 126.8	162.0 162.0	0.87	1.04
Viscount 700	29300	24500	As above	24 × 7.25	36 × 10.75	1840 2190	5210 6220	24.6 69.7	206.6 206.6	231.2 276.3	0.96	0.96
Boeing 727 SRS 100A	64400	61200	As above	32 × 11.5	49 × 17	4590 4830	13010 13690	110.5 110.5	326.7 326.7	437.2 437.2	0.69	0.73
Boeing 727 SRS 200	76700	67100	As above	32 × 11.5	49 × 17	5040 5750	14270 16290	110.5 110.5	326.7 326.7	437.2 437.2	0.58	0.66
Boeing 737 SRS 100	44000	43100	As above	24 × 7.7	40 × 14	3230 3300	9160 9350	74.0 74.0	269.0 269.0	343.0 343.0	0.79	0.81
Boeing 737 SRS 200	48500	44000	As above	24 × 7.7	40 × 14	3300 3640	9350 10310	74.0 74.0	269.0 269.0	343.0 343.0	0.72	0.79

Table 5 (continued)

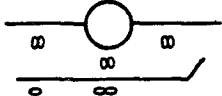
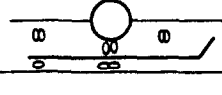
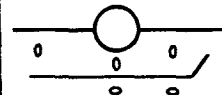
Aircraft	Maximum aircraft mass		Undercarriage type	Tyre sizes		Dynamic wheel loads		Calculated drag		Total drag kN	Retardation G	
	Take-off kg	Landing kg		Nose wheel	Main wheel	Nose kg	Main kg	Nose unit kN	Main unit kN		Take-off mass	Landing mass
Super VC 10	151900	107500		39 x 13	50 x 18	5910	11960	124.9	345.9	470.8	0.32	0.45
						8360	16900	124.9	345.9	470.8		
Boeing 707 SRS 120B	116600	86200	As above	39 x 13	46 x 16	6460 8740	9160 12390	124.9 124.9	307.4 307.4	432.3 432.3	0.38	0.51
Boeing 707 SRS 320C	150100	112000	As above	39 x 13	46 x 16	8400 11260	11900 15950	124.9 124.9	307.4 307.4	432.3 432.3	0.29	0.39
720 Boeing 720 720B	103900	79400	As above	34 x 9.9	40 x 14	7770	11030	95.1	269.0	364.1	0.36	0.47
	106100	79400				5950 7960	8430 11280	95.1 95.1	269.0 269.0	364.1 364.1		
Brittania	83900	63500		32 x 8.8	40 x 12	4760	6750	84.5	230.6	315.1	0.38	0.51
						6290	8920	84.5	230.6	315.1		
CV880 SRS 22	83700	62100	As above	29 x 7.7	39 x 13	3420 4600	6910 9310	74.0 74.0	250.0 250.0	324.0 324.0	0.39	0.53
CV880 SRS 22M	87500	70300	As above	29 x 7.7	39 x 13	3870 4820	7820 9740	74.0 74.0	250.0 250.0	324.0 324.0	0.38	0.47
CV990A	114800	91600	As above	29 x 7.7	41 x 15	5040 6310	10190 12770	74.0 74.0	288.2 288.2	362.2 362.2	0.32	0.40
DC 8 SRS 10	123800	87500	As above	34 x 11	44 x 16	6570 9290	9300 13160	105.7 105.7	307.4 307.4	413.1 413.1	0.34	0.48
DC 8 Super 63	158800	111100	As above	34 x 11	44 x 16	8340 11910	11810 37190	105.7 105.7	307.4 307.4	413.1 413.1	0.27	0.38
DC 3	11400	10900		-	45 x 17	-	5440	-	37.7	37.7	0.38	0.35
						-	5700	-	42.1	42.1		

Table 5 (concluded)

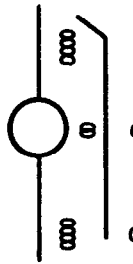
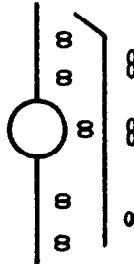
Aircraft	Maximum aircraft mass		Undercarriage type	Tyre sizes		Dynamic wheel loads		Calculated drag		Total drag kN	Retardation G	
	Take-off kg	Landing kg		Nose wheel	Main wheel	Nose kg	Main kg	Nose unit kN	Main unit kN		Take-off mass	Landing mass
Trident 2E	65100	51300		29 x 8	35 x 10	3840	5450	76.9	384.3	461.2	0.72	0.92
Boeing 747	322000	255800		46 x 16	14070	14230	153.7	614.9	768.6	0.24	0.31	
												17710

Table 6

DETAILS OF AIRCRAFT OPERATING AT 'HONG KONG' AND THEIR CALCULATED DRAG AND MEAN RETARDATION IN A PLASTIC FOAM
ARRESTER BED 0.51m DEEP × 380kPa FOAM OVER 0.64m DEEP × 760kPa MEAN CRUSHING STRESS FOAM

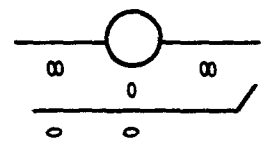
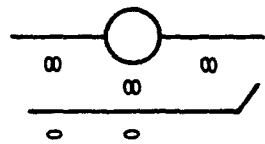
Aircraft	Maximum aircraft mass		Undercarriage type	Tyre sizes		Dynamic wheel loads		Calculated drag		Total drag kN	Retardation G	
	Take-off kg	Landing kg		Nose wheel	Main wheel	Nose kg	Main kg	Nose unit kN	Main unit kN		Take-off mass	Landing mass
DC 4	33100	28800		45 × 16.25	45 × 15.5	4320	6120	10.7	98.7	109.4	0.48	0.39
						4970	7040	14.4	140.5	154.9		
DC 9 SRS 10	35200	33600		26 × 6.6	40 × 14	2520	7130	65.9	274.1	340.0	0.99	1.03
						2640	7490	66.9	275.4	342.3		
DC 9 SRS 40	51700	46300	As above	26 × 6.6	40 × 14	3470 3880	9830 10990	82.7 99.5	321.6 372.9	404.3 472.4	0.93	0.89
DHC-4A	12900	12900	As above	24 × 7.5	32 × 11	970 970	2750 2750	4.3 4.3	37.9 37.9	42.2 42.2	0.33	0.33
Jetstream	19100	15900	As above	18 × 4.4	26 × 6.6	1190 1430	3370 4050	39.2 40.8	159.8 213.8	199.0 254.6	1.36	1.28
Viscount 700	29300	24500	As above	24 × 7.25	36 × 10.75	1840 2190	5210 6220	19.9 71.0	211.6 226.4	231.5 297.4	1.04	0.96
Boeing 727 SRS 100A	64400	61200	As above	32 × 11.5	49 × 17	4590 4830	13010 13690	112.5 112.8	359.1 374.8	471.6 487.6	0.77	0.79

Table 6 (continued)

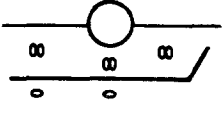
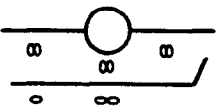
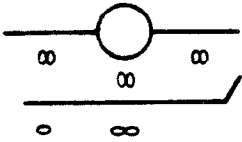
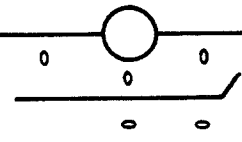
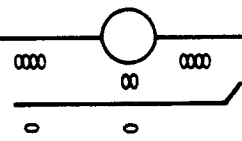
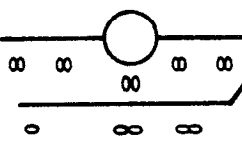
Aircraft	Maximum aircraft mass		Undercarriage type	Tyre sizes		Dynamic wheel loads		Calculated drag		Total drag kN	Retardation G	
	Take-off kg	Landing kg		Nose wheel	Main wheel	Nose kg	Main kg	Nose unit kN	Main unit kN		Take-off mass	Landing mass
Boeing 727 SRS 200	76600	67100		32 × 11.5	49 × 17	5040	14300	113.4	391.5	504.9	0.79	0.77
						5750	16290	118.4	476.5	594.9		
Boeing 737 SRS 100	44000	43000	As above	24 × 7.7	40 × 14	3230 3300	9160 9350	82.9 84.2	301.1 306.3	384.1 390.5	0.91	0.91
Boeing 737 SRS 200	48500	44000	As above	24 × 7.7	40 × 14	3300 3640	9350 10310	84.2 92.0	306.3 340.2	390.5 432.2	0.91	0.91
Super VC 10	152000	107500		39 × 13	50 × 18	5910	11960	80.0	489.5	569.5	0.61	0.54
						8360	16910	140.3	774.3	914.7		
Boeing 707 SRS 120B	116600	86200	As above	39 × 13	46 × 16	6460 8740	9160 12390	127.2 146.1	313.1 547.0	440.4 693.0	0.61	0.52
Boeing 707 SRS 320C	150000	112000	As above	39 × 13	46 × 16	8400 11260	11900 15950	141.0 220.2	517.4 814.2	658.4 1034.4	0.70	0.60
720 Boeing 720 720B	103900	79400	As above	34 × 9.9	40 × 14	7770	11030	176.3	587.6	763.9	0.75	0.65
	106100	79400				5950 7960	8430 11280	111.9 188.4	397.0 614.2	508.9 802.6		
Brittania	83900	63500	As above	32 × 8.8	40 × 12	4760 6290	6750 8920	95.1 139.7	320.3 451.0	415.4 590.7	0.72	0.67
CV880 SRS 22	83700	62100	As above	29 × 7.7	39 × 13	3420 4600	6910 9310	78.2 101.8	337.2 473.5	415.4 575.3	0.70	0.68
CV880 SRS 22M	87500	70700	As above	29 × 7.7	39 × 13	3870 4800	7820 9740	83.9 109.8	374.8 512.5	458.7 622.3	0.72	0.67
CV990A	114800	91600	As above	29 × 7.7	41 × 15	5040 6310	10190 12770	120.4 169.5	479.0 713.6	599.4 883.1	0.78	0.67

Table 6 (concluded)

Aircraft	Maximum aircraft mass		Undercarriage type	Tyre sizes		Dynamic wheel loads		Calculated drag		Total drag kN	Retardation G	
	Take-off kg	Landing kg		Nose wheel	Main wheel	Nose kg	Main kg	Nose unit kN	Main unit kN		Take-off mass	Landing mass
DC 8 SRS 10	123800	87500		34 × 11	44 × 16	6560	9300	123.5	418.9	542.4	0.74	0.63
						9290	13160	262.1	637.3	899.4		
DC 8 Super 63	158800	111100	As above	34 × 11	44 × 16	8340 11910	11810 16870	177.6 269.1	534.3 814.2	711.9 1083.3	0.70	0.65
DC 3	11400	10900		-	45 × 17	-	5440	-	54.7	54.7	0.49	0.51
						-	5700	-	55.4	55.4		
Trident 2E	65090	51260		29 × 8	35 × 10	3840 4880	5450 6920	84.6 109.3	412.7 520.4	497.3 629.7	0.99	0.99
Boeing 747	322100	255800		46 × 16	46 × 16	14070	14230	211.9	1393.9	1605.8	0.64	0.64
						17710	16910	383.7	1628.3	2012.0		

REFERENCES

- | <u>No.</u> | <u>Author</u> | <u>Title, etc.</u> |
|------------|------------------------|---|
| 1 | E. Bade | Soft ground arresting of civil aircraft.
RAE Technical Report 68032 (ARC 30133) (1968) |
| 2 | E. Bade
E.M. Minter | Soft ground arresting of civil aircraft -
scaled model VC 10 tests in gravel and sintered
fuel ash pellets.
RAE Technical Report 71015 (ARC 33068) (1971) |
| 3 | T.G. Randall | Preliminary feasibility study of the arresting of
aircraft in a foamed plastic overrun area.
RAE Technical Memorandum Naval 213 (1970) |
| 4 | G.M. Gwynne | Use of foamed plastics as emergency aircraft arresters.
Study of the arresting effects for different groups
of aircraft on selected runways.
RAE Technical Memorandum Naval 217 (ARC 34763) (1972) |

Examples of wheel rolling conditions in foam used in calculations of foam upthrust pressure and drag

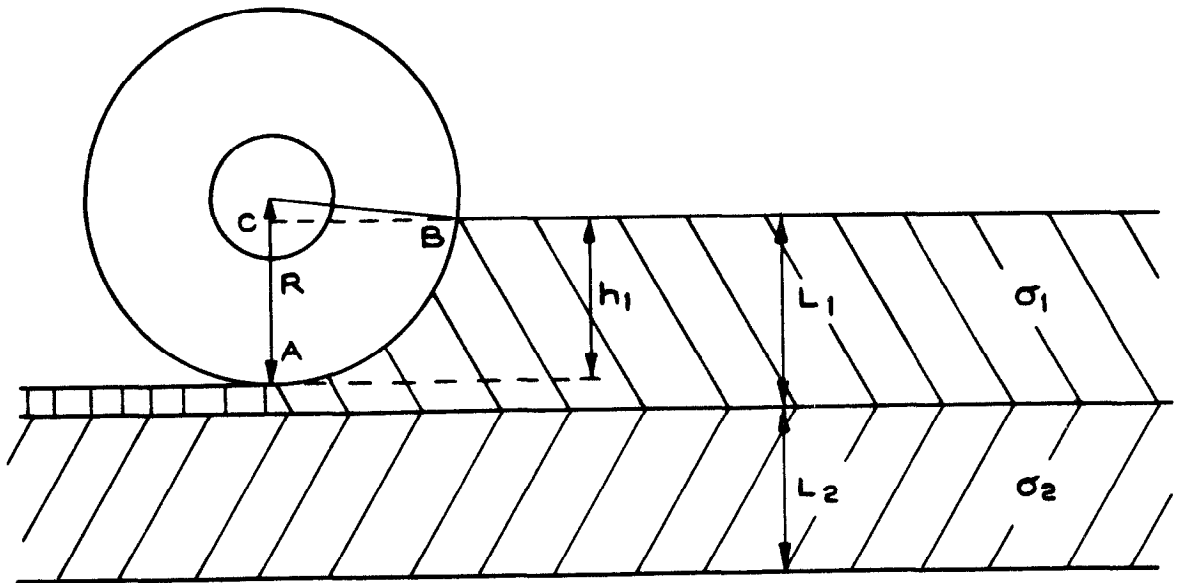


Fig.1 Wheel supported by the upper foam layer

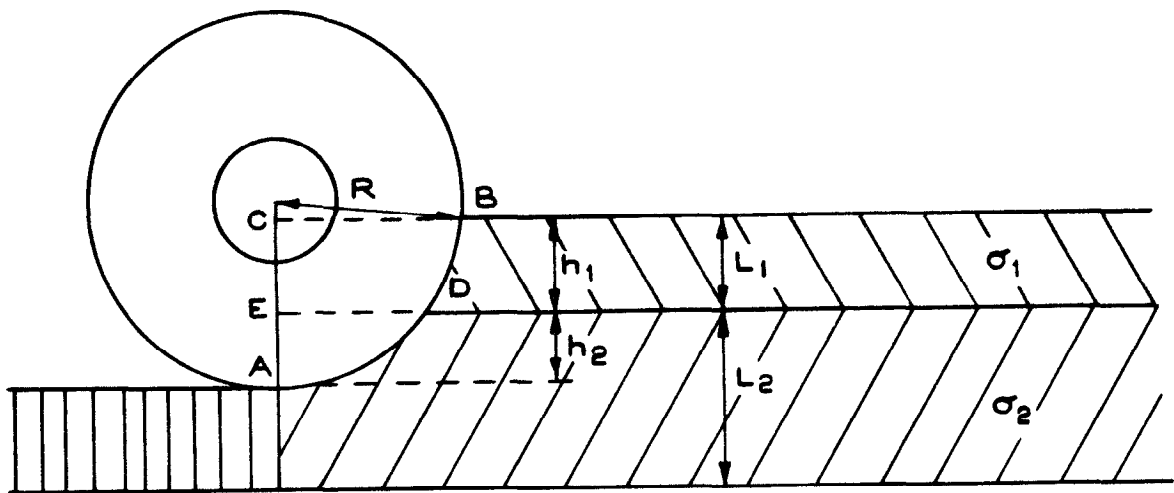


Fig.2 Wheel supported by both foam layers and protruding above the upper layer

Examples of wheel rolling conditions in foam used in calculations of foam upthrust pressure and drag

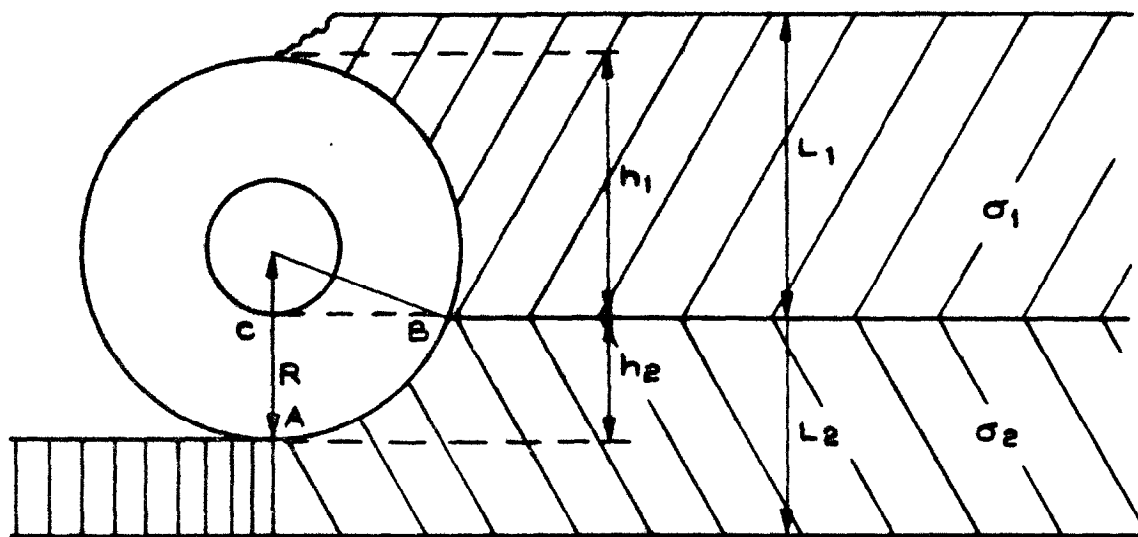


Fig.3 Wheel completely embedded in both foam layers

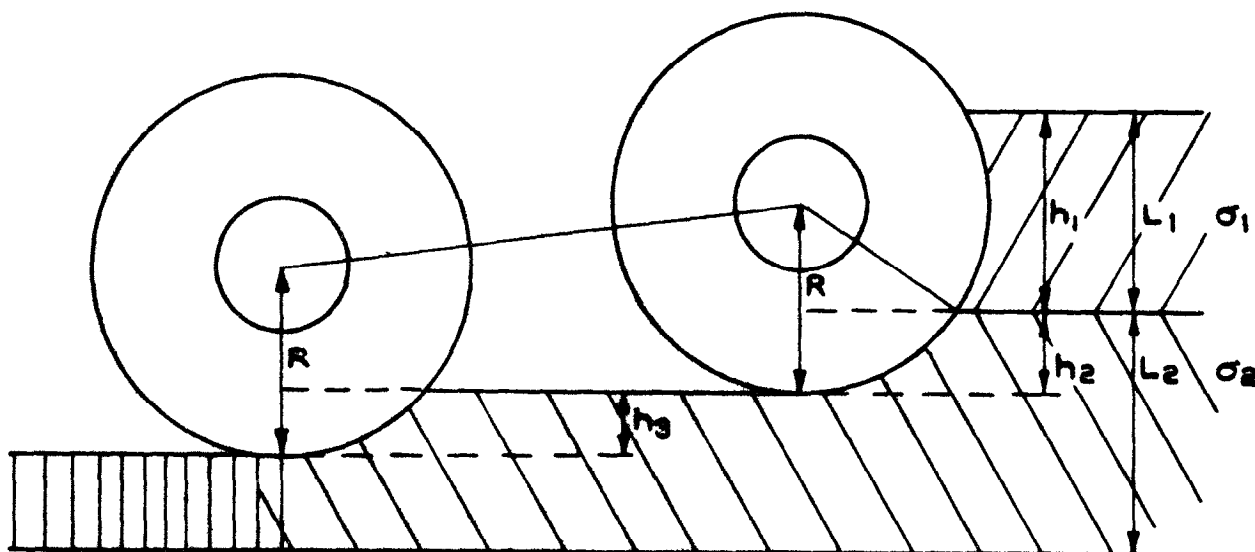


Fig.4 Bogie wheels in foam



Fig.5 Arrangement of the single layered UF foam test beds used for trials



Fig.6 Arrangement of the double layered UF foam test beds used for trials

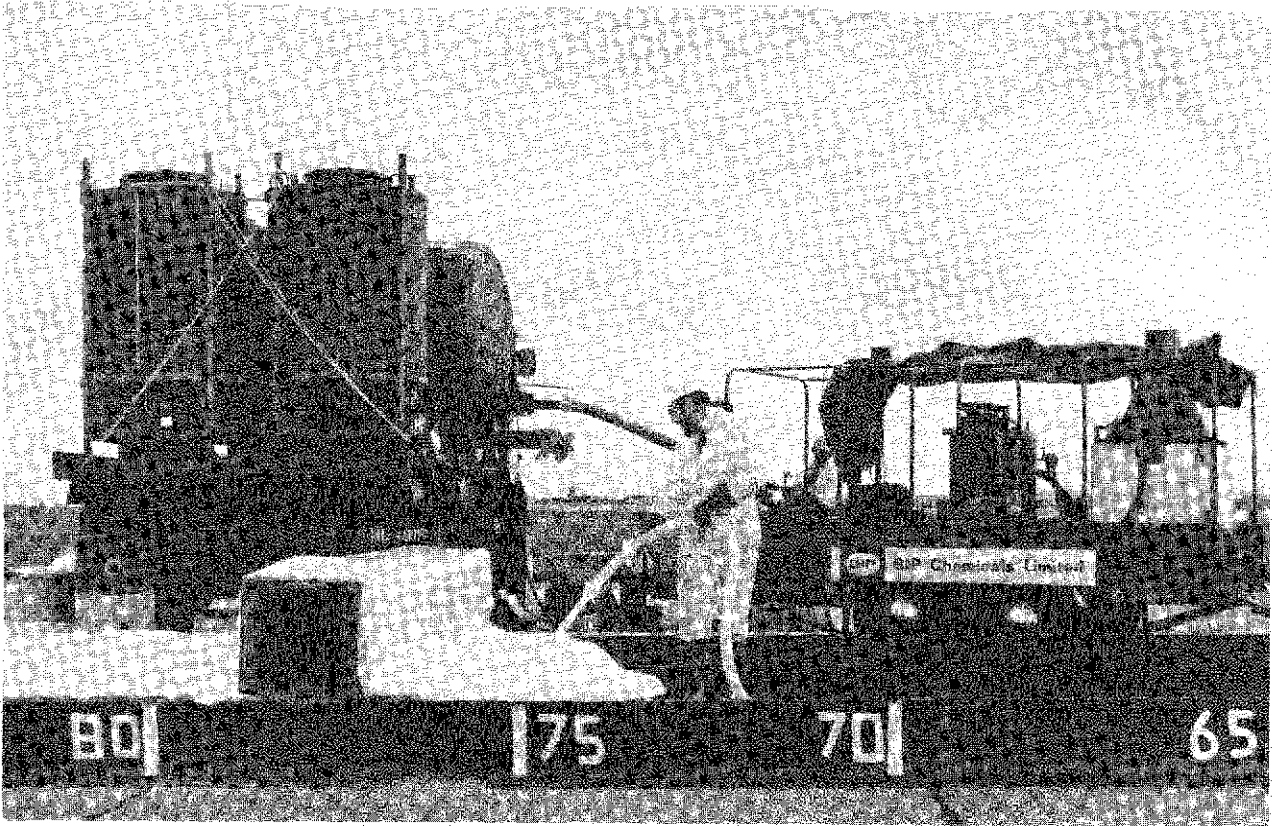


Fig.7 Equipment used, and method employed during foam laying

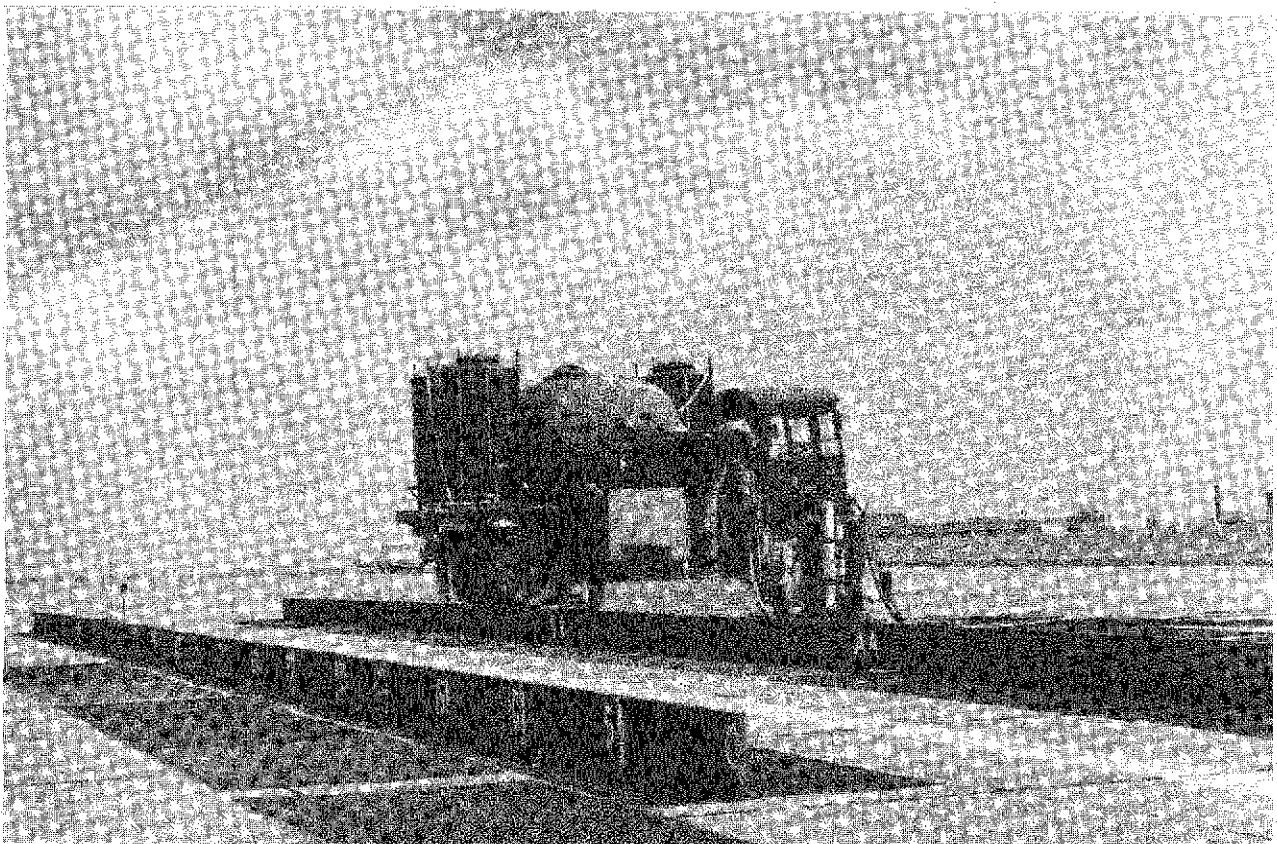


Fig.8 Arrangement of steel wire mesh used to key UF foam to the runway surface



Fig.9 Method employed to measure mean foam crushing strength values

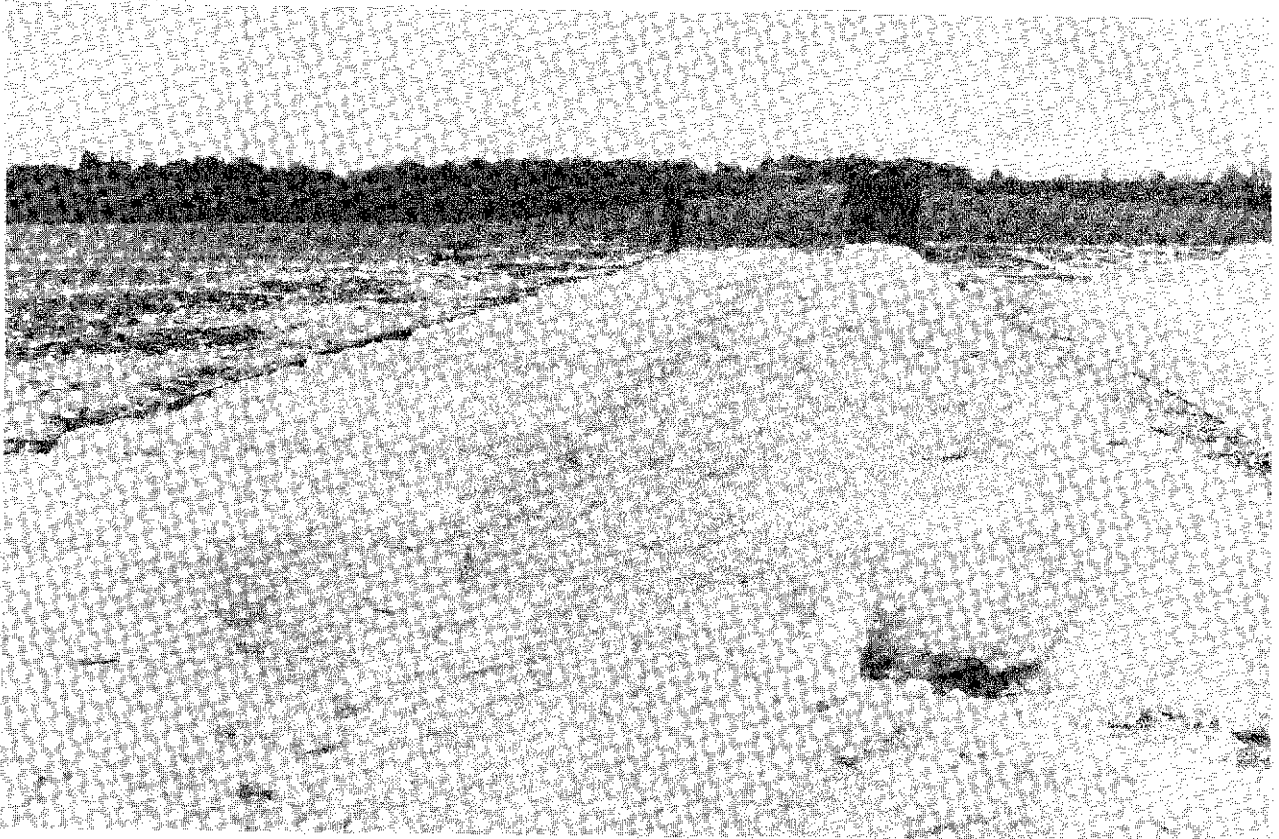


Fig.10 Furrow formed by a main undercarriage wheel unit

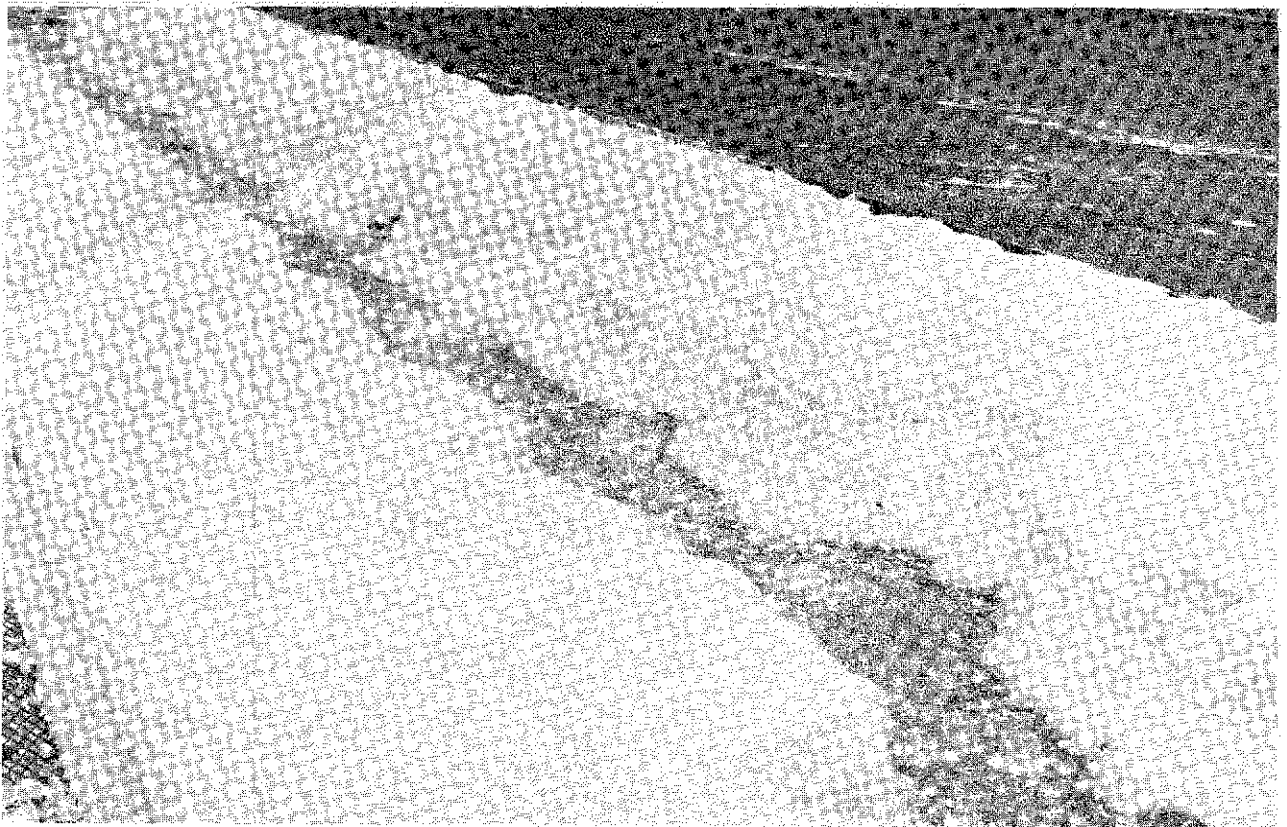


Fig.11 UF foam pad prepared for refilling

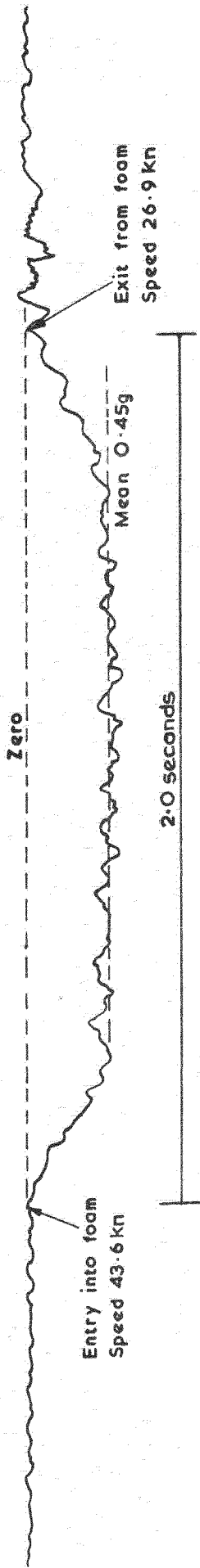


Fig.12 Retardation trace during an unbraked engagement. (Run 4)

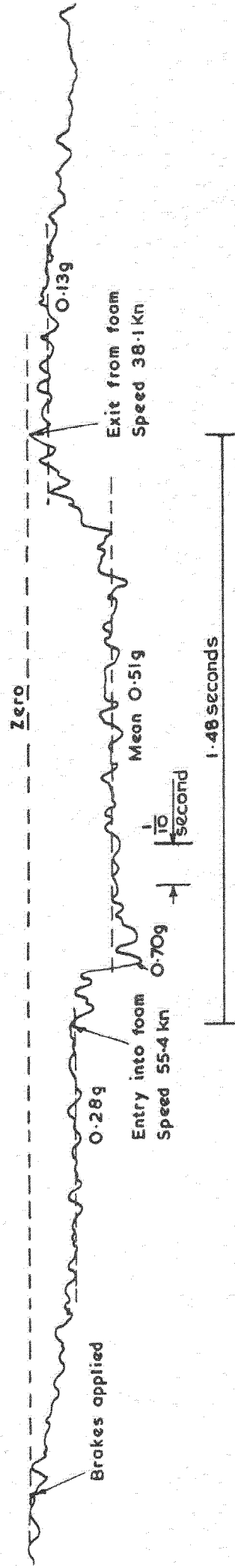


Fig.13 Retardation trace during a 'brakes on' engagement. (Run 5)

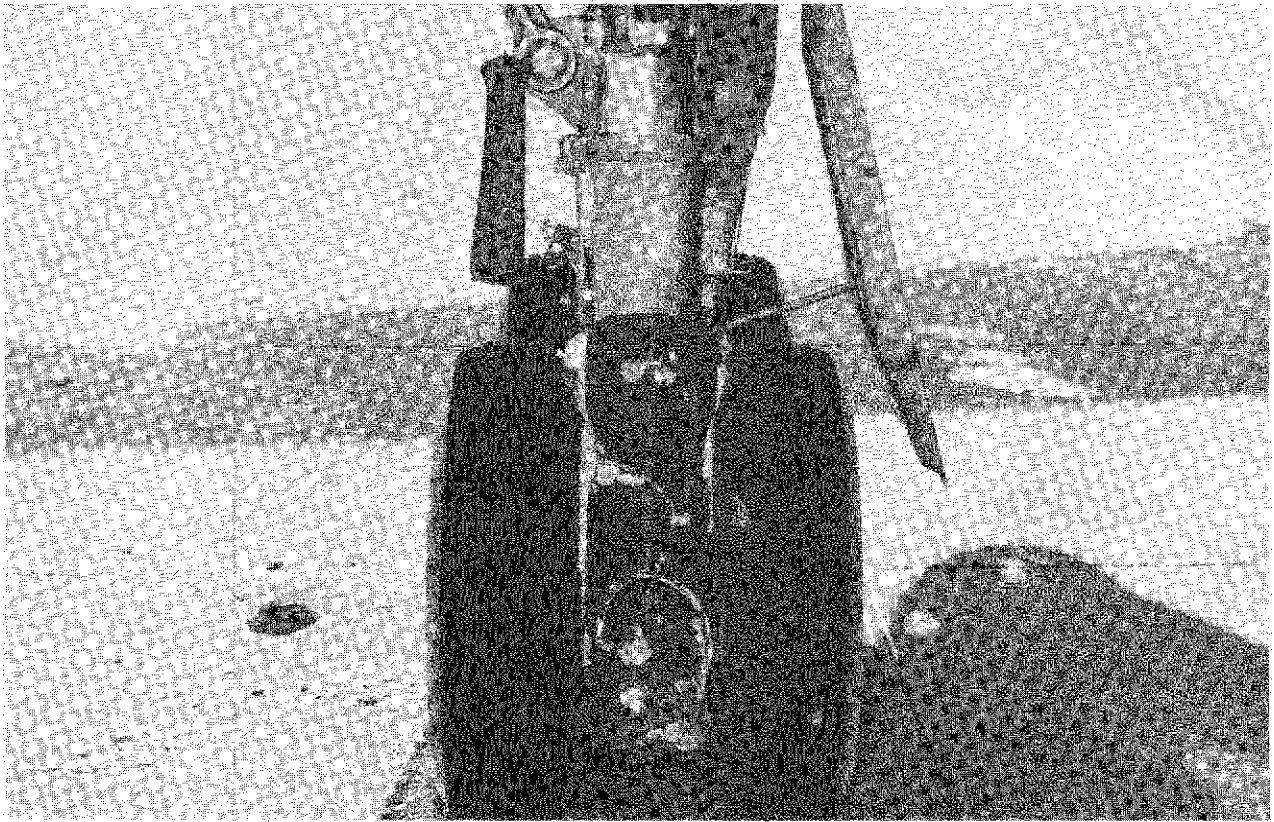


Fig.14 View of protective plate after an arrest

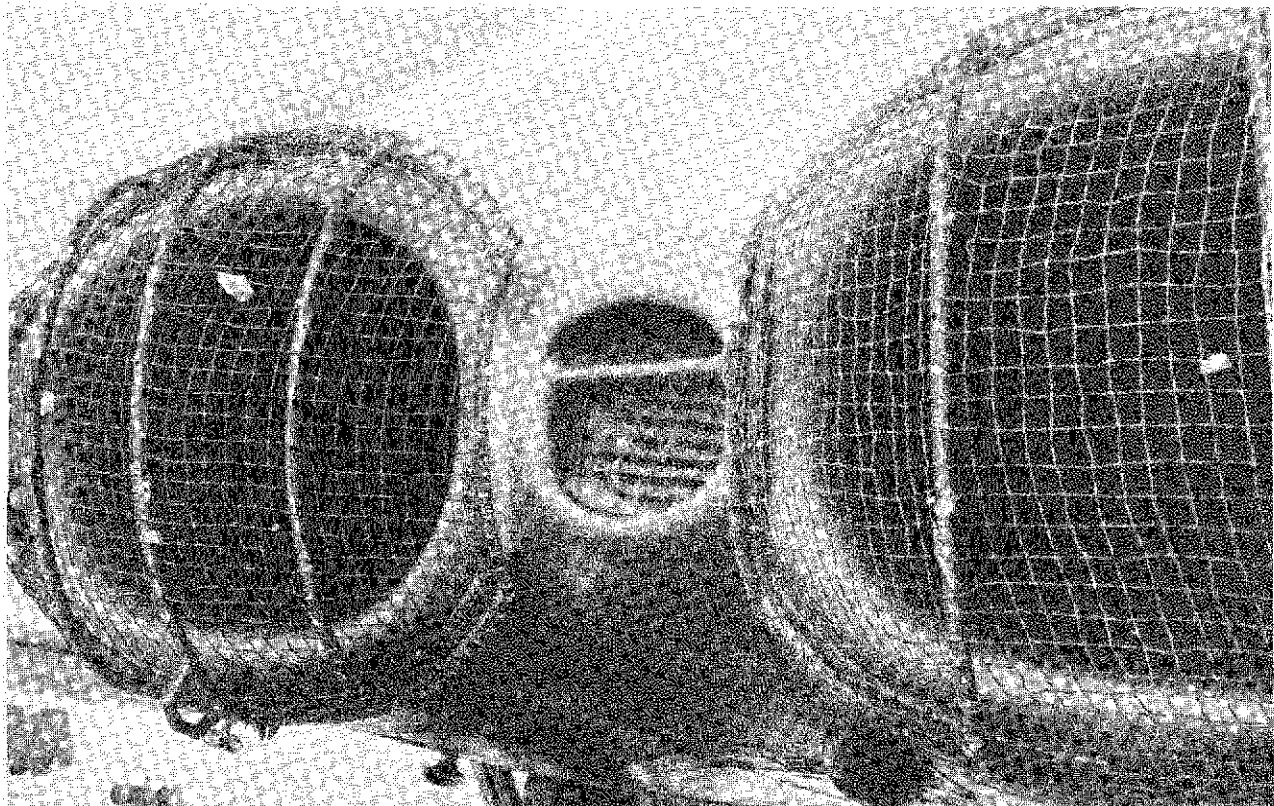


Fig.15 Wire mesh guards fitted over the Comet engines air intakes

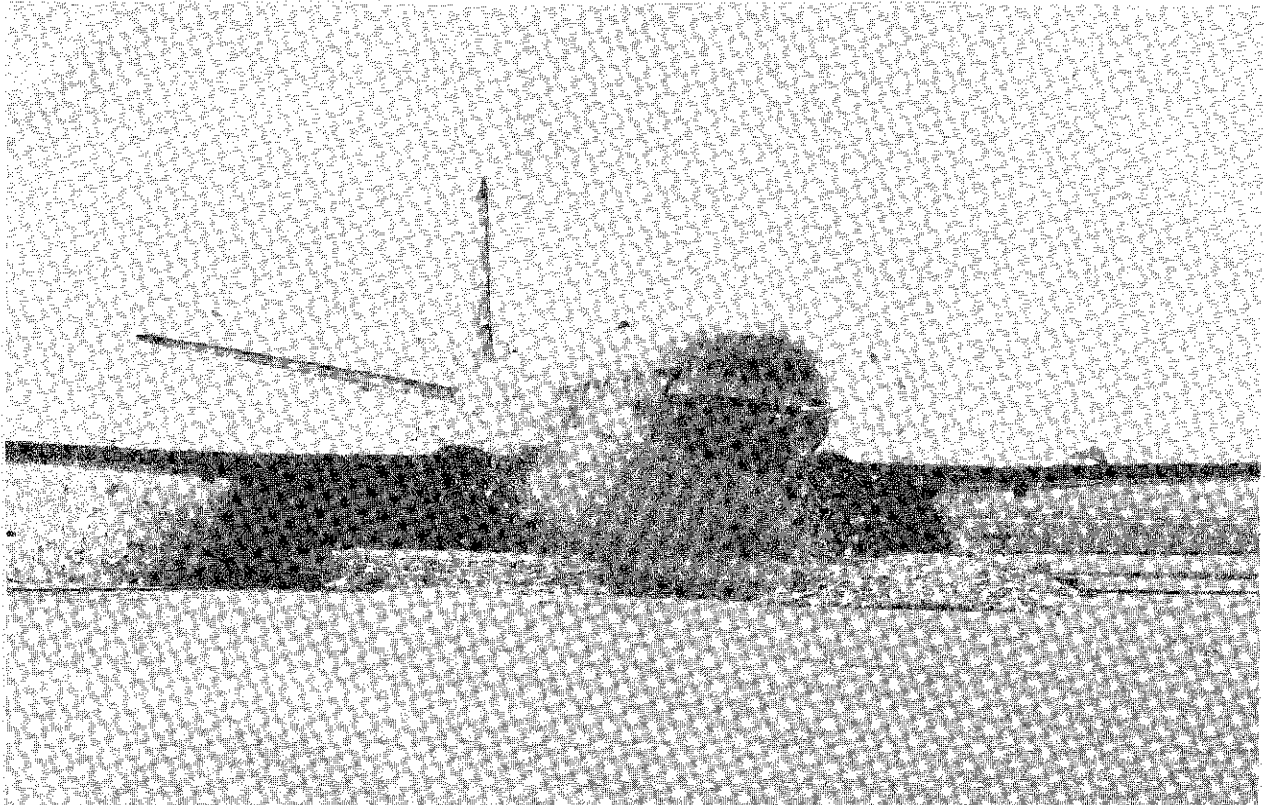


Fig.16 View of foam spray around air intakes during an arrest

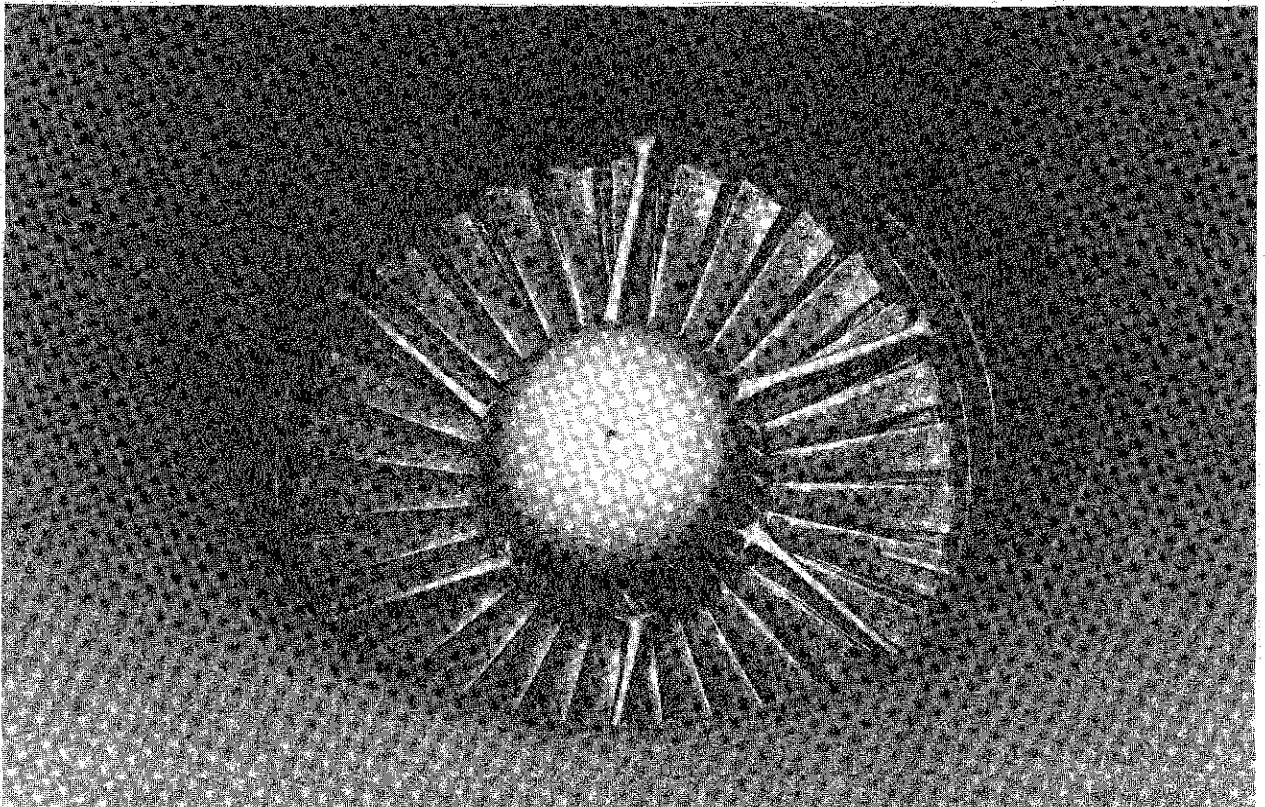


Fig.17 Foam deposits on engine inlet guide vanes after an arrest

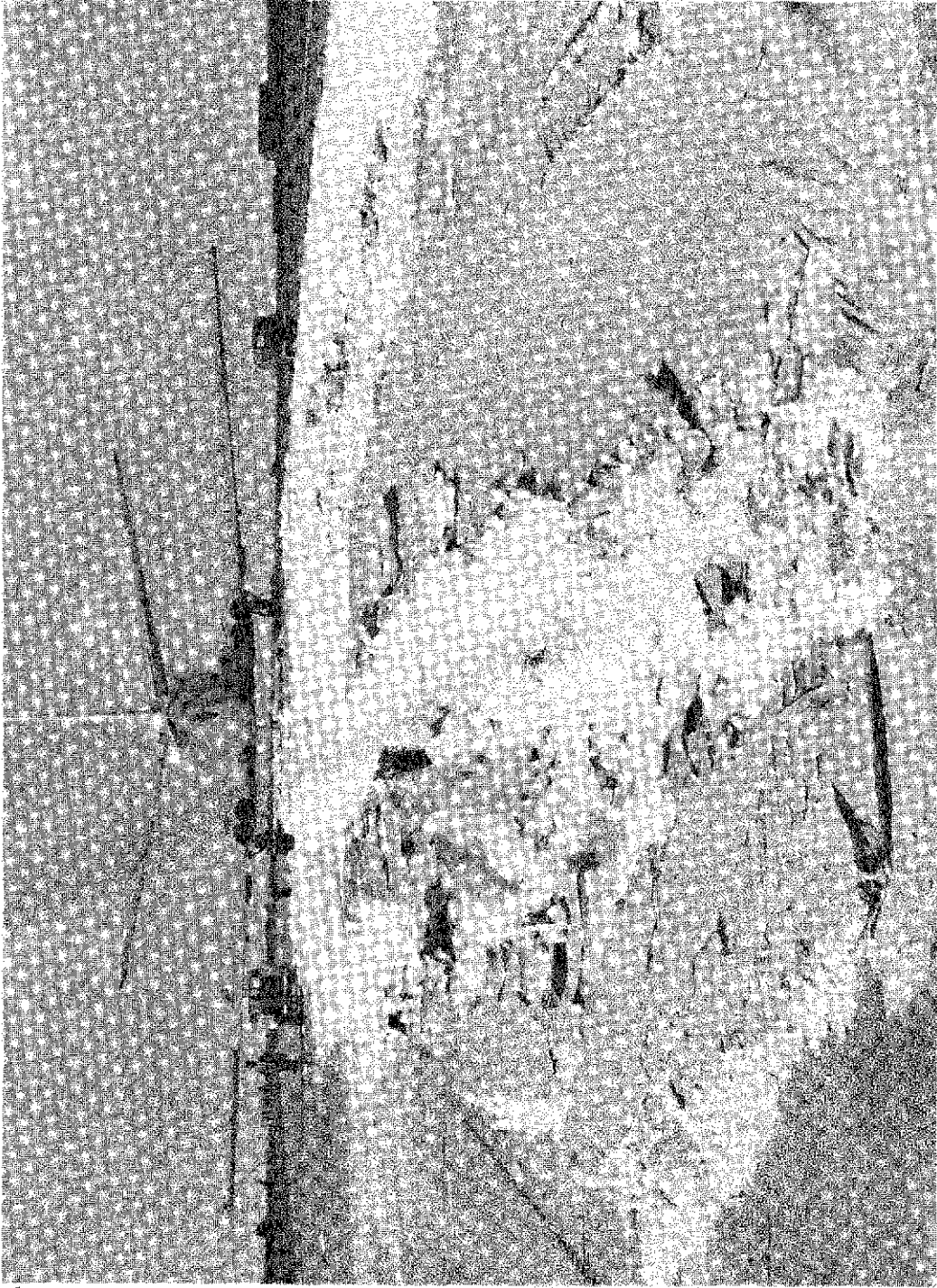


Fig. 18 View of the port foam arrester edge after the off centre engagement

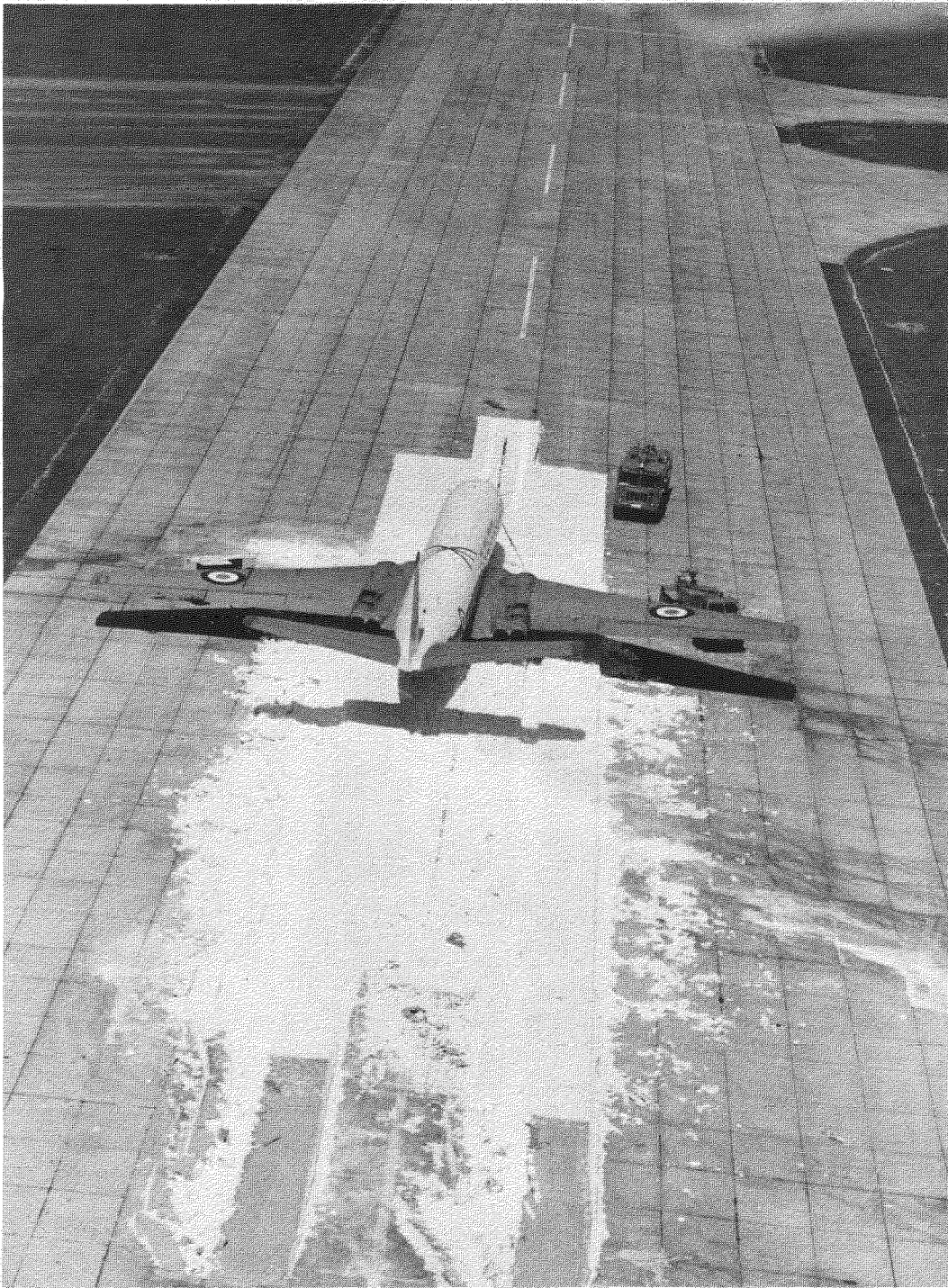


Fig.19 Aerial view of the Comet arrested in UF foam

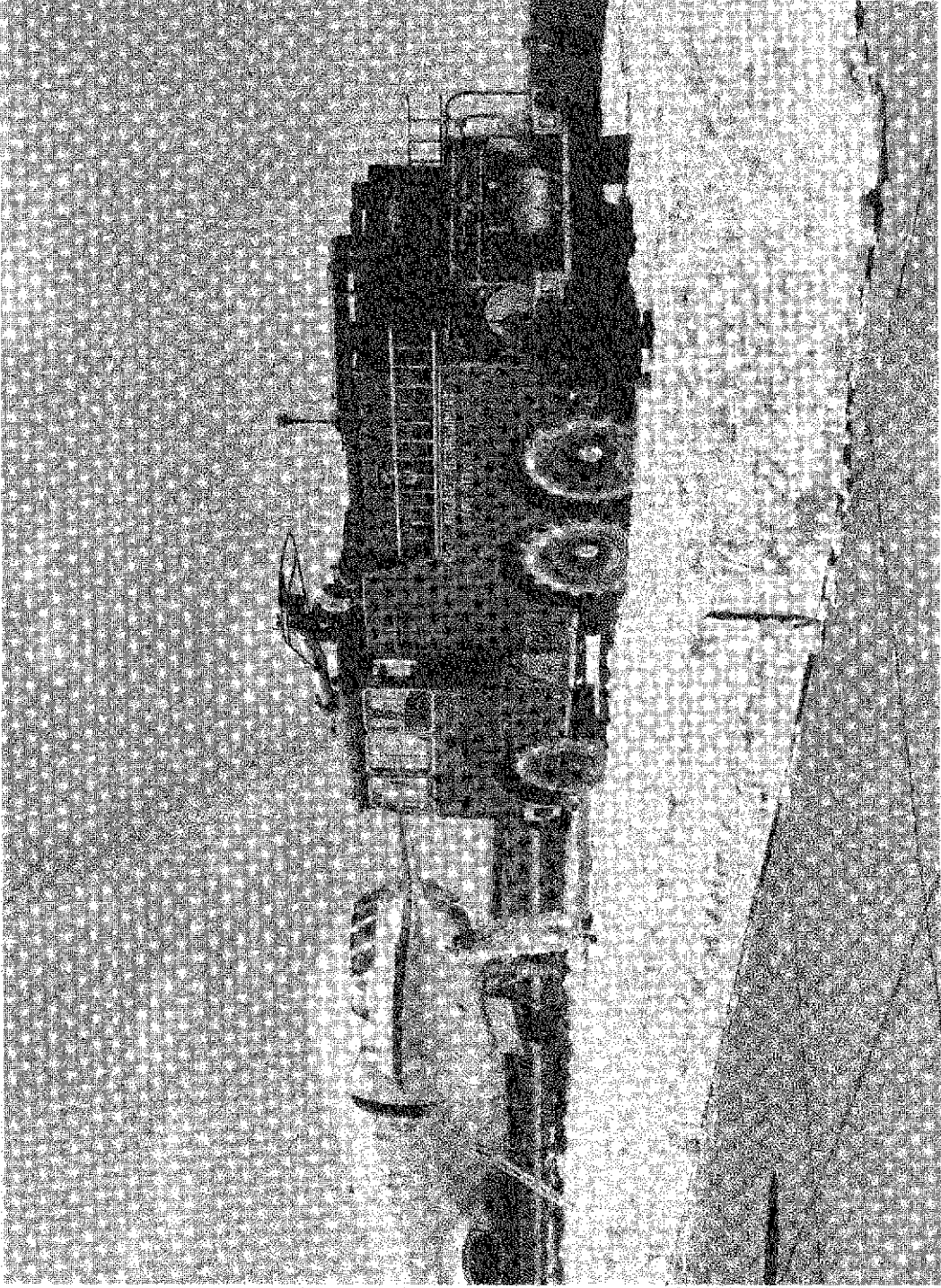


Fig.20 Nubian Major fire fighting foam tender approaching arrested Comet

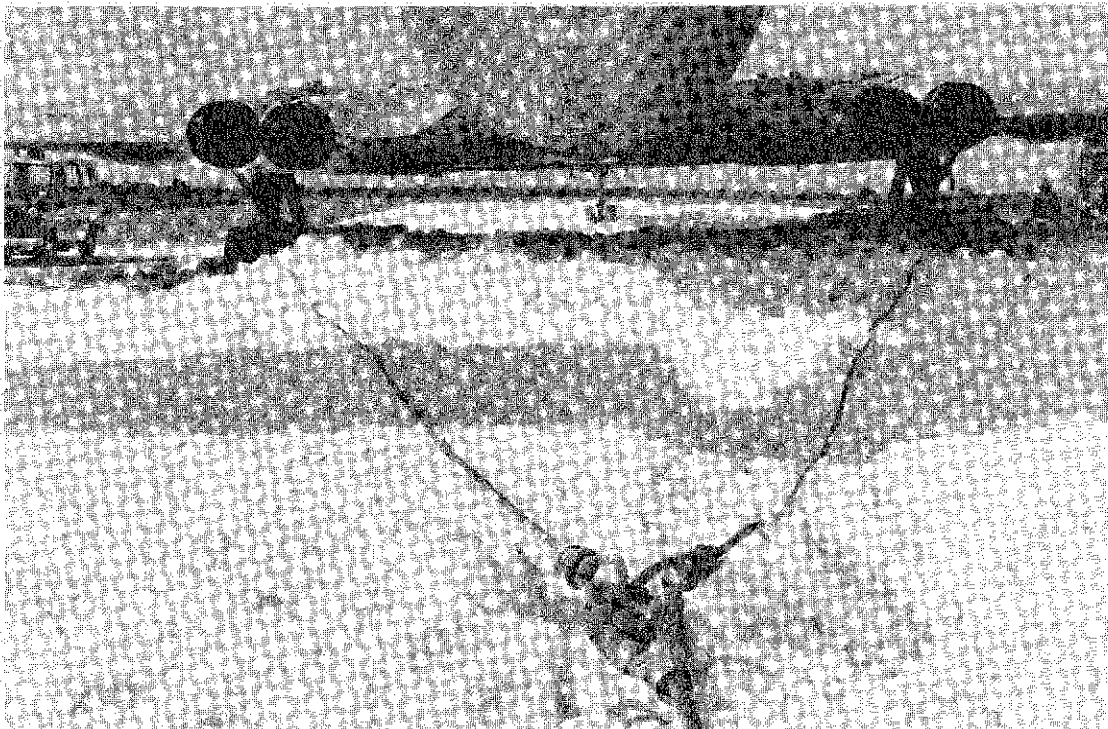


Fig.21 Arrangement of the steel wire ropes attached for removing the Comet

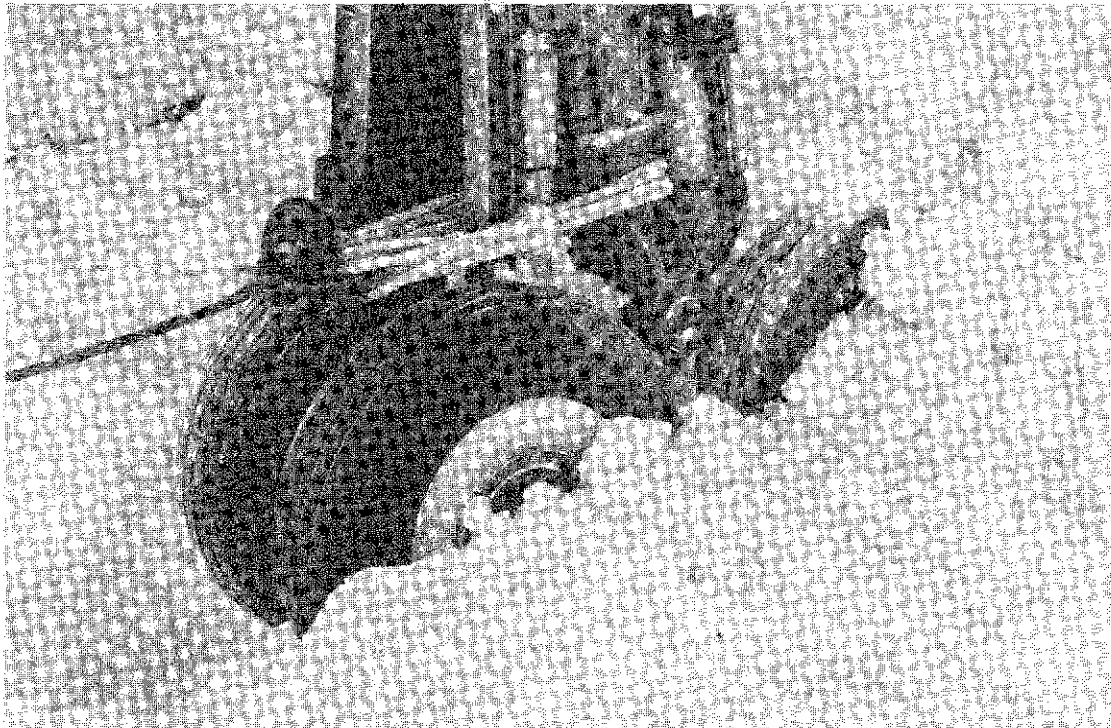


Fig.22 Method employed for attaching the steel wire rope to a main undercarriage wheel unit

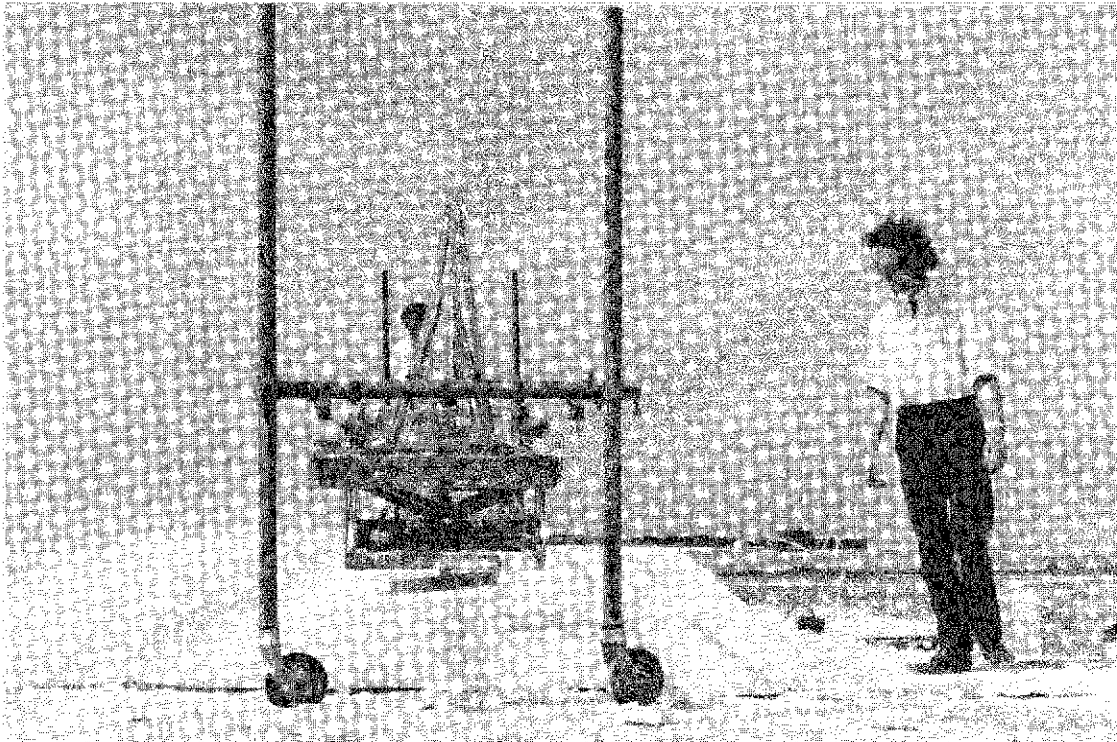


Fig.23 Milling of foam arrester surface prior to sealing and weather-proofing

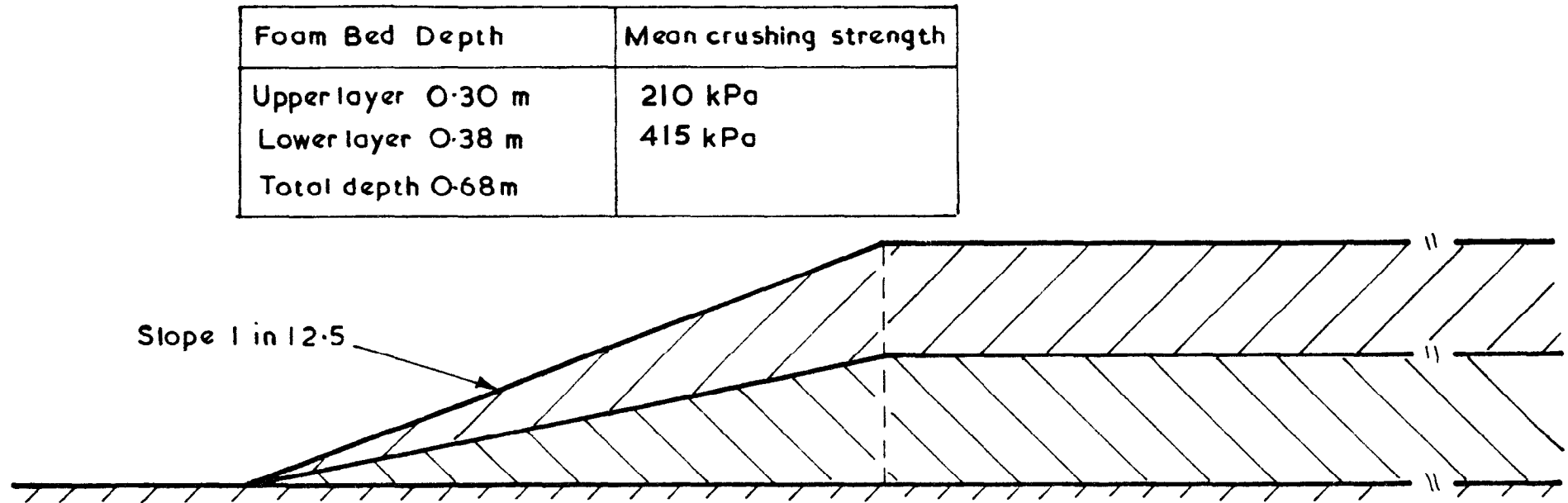


Fig.24 Details of foamed plastic arrester for United Kingdom airfields

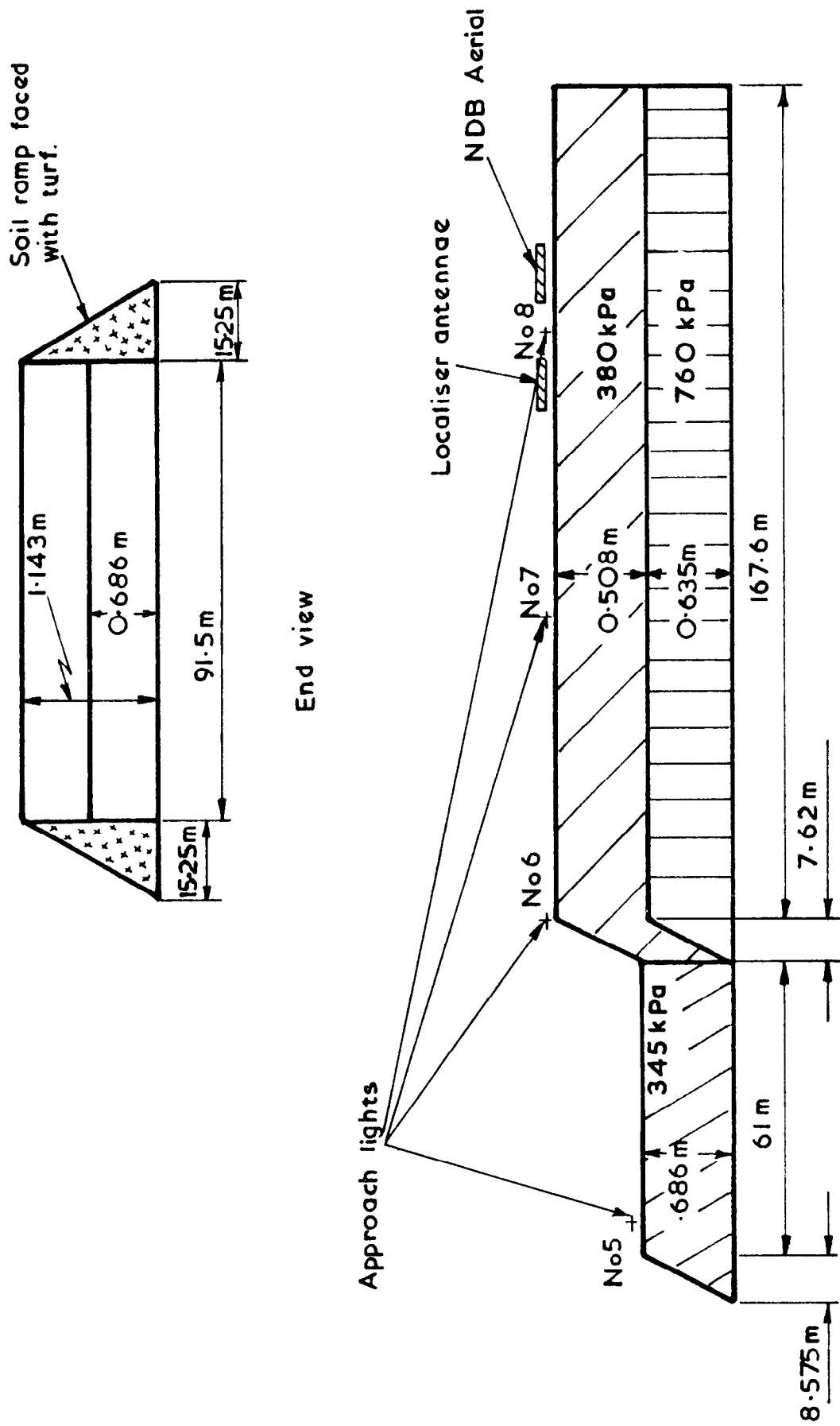
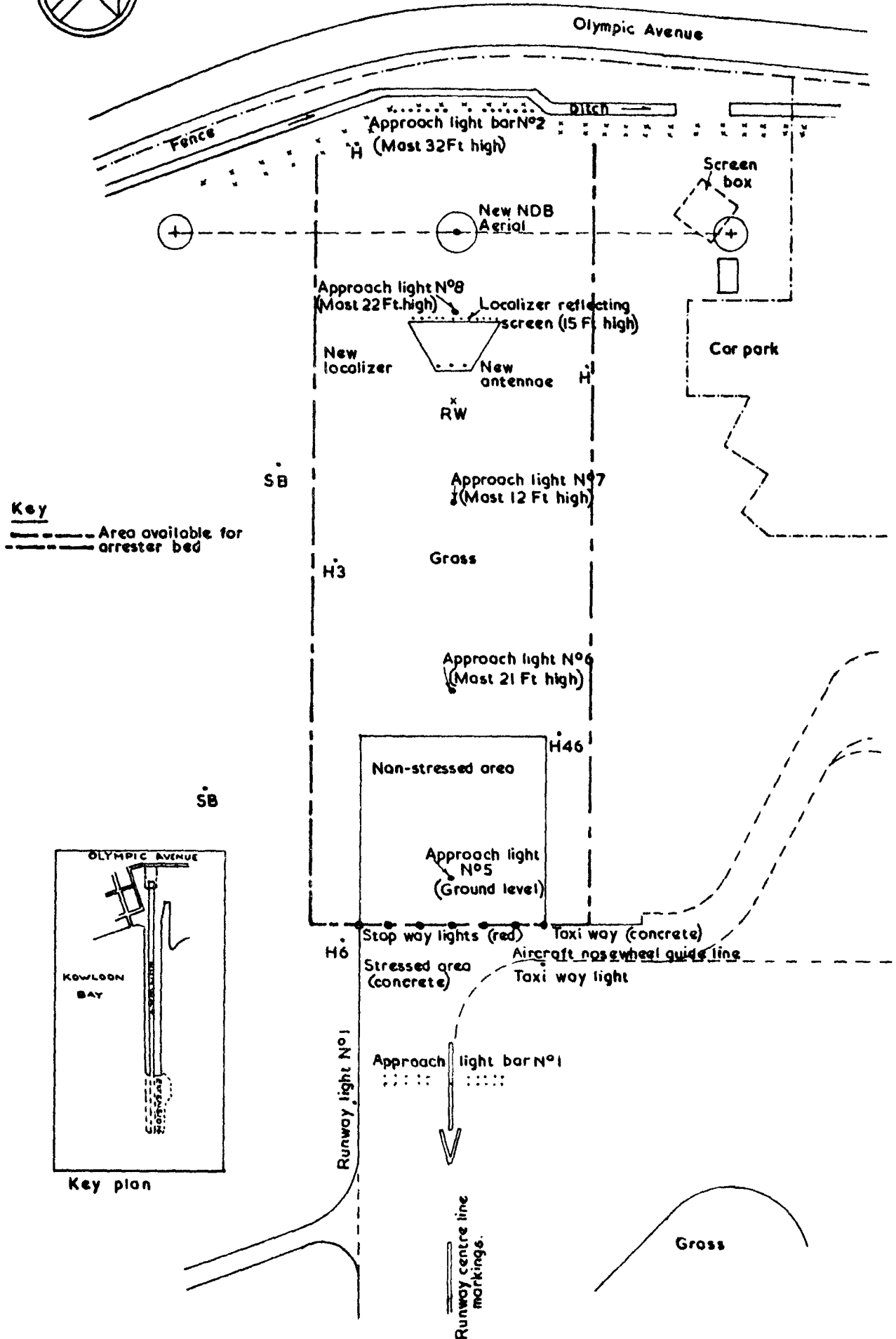


Fig.25 Details of the UF foamed plastic arrester for Hong Kong



T.R.74002

Fig.26 Civil Aviation Department Hong Kong Kai Tak Airport

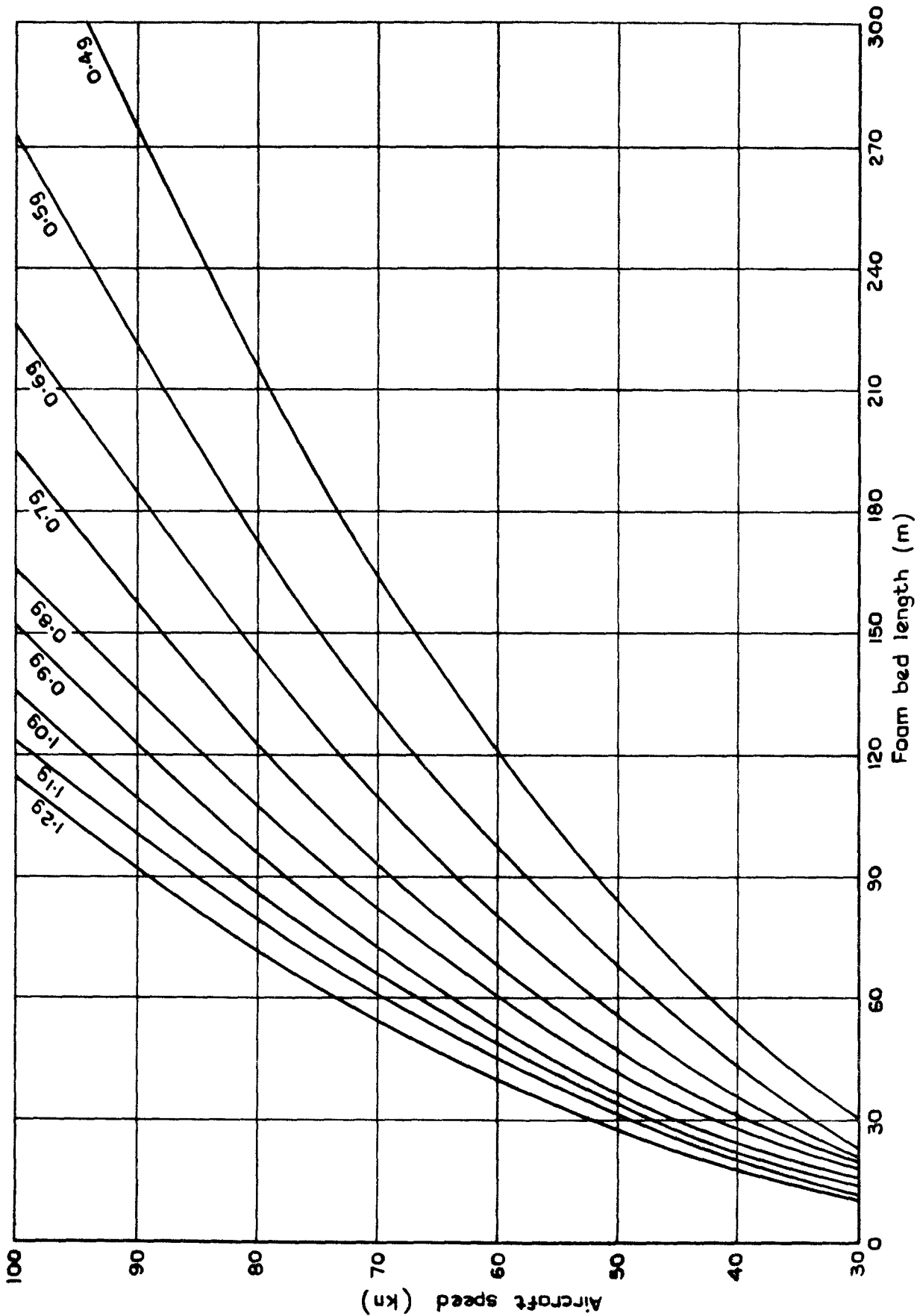


Fig.27 Relationship between engaging speeds and foam arrester lengths for various values of retardation

ARC CP No.1329
January 1974

629.13.015.981.1 :
678.5-496 :
678.6'41

Gwynne, G. M.

**UREA FORMALDEHYDE FOAMED PLASTIC
EMERGENCY ARRESTERS FOR CIVIL AIRCRAFT**

This Report describes arresting trials with a Comet 3B aircraft at its maximum landing mass of 54400 kg at speeds up to 56 kn in test beds of urea formaldehyde foam of varying depth, length and density.

The main conclusions from the trials are that retardation of the aircraft in the arrester is independent of entry speed; significant drag is contributed by both the leading and trailing wheels of a bogie arrangement and this drag is predictable; the performance of the arrester is unaffected by the application of anti skid controlled wheel brakes; the foam causes no significant damage to turbine engines or aircraft structure; and the addition of a foam lead-in gradient to the full depth foam bed reduces the ratio of peak to mean retardation. A number of minor conclusions are also presented.

The Report includes design examples for foam arresters demonstrating that it should be possible to devise configurations, suitable for airfields where overrun hazards exist, for arresting aircraft safely without overstressing undercarriage units due to the foam drag loads.

ARC CP No.1329
January 1974

629.13.015.981.1 :
678.5-496 :
678.6'41

Gwynne, G. M.

**UREA FORMALDEHYDE FOAMED PLASTIC
EMERGENCY ARRESTERS FOR CIVIL AIRCRAFT**

This Report describes arresting trials with a Comet 3B aircraft at its maximum landing mass of 54400 kg at speeds up to 56 kn in test beds of urea formaldehyde foam of varying depth, length and density.

The main conclusions from the trials are that retardation of the aircraft in the arrester is independent of entry speed; significant drag is contributed by both the leading and trailing wheels of a bogie arrangement and this drag is predictable; the performance of the arrester is unaffected by the application of anti skid controlled wheel brakes; the foam causes no significant damage to turbine engines or aircraft structure; and the addition of a foam lead-in gradient to the full depth foam bed reduces the ratio of peak to mean retardation. A number of minor conclusions are also presented.

The Report includes design examples for foam arresters demonstrating that it should be possible to devise configurations, suitable for airfields where overrun hazards exist, for arresting aircraft safely without overstressing undercarriage units due to the foam drag loads.

DETACHABLE ABSTRACT CARDS

ARC CP No.1329
January 1974

629.13.015.981.1 :
678.5-496 :
678.6'41

Gwynne, G. M.

**UREA FORMALDEHYDE FOAMED PLASTIC
EMERGENCY ARRESTERS FOR CIVIL AIRCRAFT**

This Report describes arresting trials with a Comet 3B aircraft at its maximum landing mass of 54400 kg at speeds up to 56 kn in test beds of urea formaldehyde foam of varying depth, length and density.

The main conclusions from the trials are that retardation of the aircraft in the arrester is independent of entry speed; significant drag is contributed by both the leading and trailing wheels of a bogie arrangement and this drag is predictable; the performance of the arrester is unaffected by the application of anti skid controlled wheel brakes; the foam causes no significant damage to turbine engines or aircraft structure; and the addition of a foam lead-in gradient to the full depth foam bed reduces the ratio of peak to mean retardation. A number of minor conclusions are also presented.

The Report includes design examples for foam arresters demonstrating that it should be possible to devise configurations, suitable for airfields where overrun hazards exist, for arresting aircraft safely without overstressing undercarriage units due to the foam drag loads.

ARC CP No.1329
January 1974

629.13.015.981.1 :
678.5-496 :
678.6'41

Gwynne, G. M.

**UREA FORMALDEHYDE FOAMED PLASTIC
EMERGENCY ARRESTERS FOR CIVIL AIRCRAFT**

This Report describes arresting trials with a Comet 3B aircraft at its maximum landing mass of 54400 kg at speeds up to 56 kn in test beds of urea formaldehyde foam of varying depth, length and density.

The main conclusions from the trials are that retardation of the aircraft in the arrester is independent of entry speed; significant drag is contributed by both the leading and trailing wheels of a bogie arrangement and this drag is predictable; the performance of the arrester is unaffected by the application of anti skid controlled wheel brakes; the foam causes no significant damage to turbine engines or aircraft structure; and the addition of a foam lead-in gradient to the full depth foam bed reduces the ratio of peak to mean retardation. A number of minor conclusions are also presented.

The Report includes design examples for foam arresters demonstrating that it should be possible to devise configurations, suitable for airfields where overrun hazards exist, for arresting aircraft safely without overstressing undercarriage units due to the foam drag loads.

DETACHABLE ABSTRACT CARDS

--- Cut here ---

--- Cut here ---

C.P. No. 1329

© *Crown copyright*

1975

Published by
HER MAJESTY'S STATIONERY OFFICE

Government Bookshops

49 High Holborn, London WC1V 6HB

13a Castle Street, Edinburgh EH2 3AR

41 The Hayes, Cardiff CF1 1JW

Brazennose Street, Manchester M60 8AS

Southey House, Wine Street, Bristol BS1 2BQ

258 Broad Street, Birmingham B1 2HE

80 Chichester Street, Belfast BT1 4JY

*Government Publications are also available
through booksellers*

C.P. No. 1329

ISBN 011 470939 4